2D Thaw Lake Modelling during the Holocene and Implications for Current Climatic Change

Alana Haysom, Honours Thesis
Supervisor: Dr. Lawrence J. Plug

Submitted in Partial Fulfilment of the Requirements
For the Degree of Bachelor of Science, Honours
Department of Earth Sciences
Dalhousie University, Halifax, Nova Scotia
March 2007

DALHOUSIE UNIVERSITY
Inspiring Minds

Department of Earth Sciences
Halifax, Nova Scotia
Canada B3H 4J1
(902) 494-2358
FAX (902) 494-6889

DATE: April 27th 1007

AUTHOR: Alana K Haysom

TITLE: 2D Thermo Lake Modelling during the Holocene and Implications for Current Climate Change

Degree: BSc Convocation: May Year: 2007

Permission is herewith granted to Dalhousie University to circulate and to have copied for non-commercial purposes, at its discretion, the above title upon the request of individuals or institutions.

Signature of Author

THE AUTHOR RESERVES OTHER PUBLICATION RIGHTS, AND NEITHER THE THESIS NOR EXTENSIVE EXTRACTS FROM IT MAY BE PRINTED OR OTHERWISE REPRODUCED WITHOUT THE AUTHOR'S WRITTEN PERMISSION.

THE AUTHOR ATTESTS THAT PERMISSION HAS BEEN OBTAINED FOR THE USE OF ANY COPYRIGHTED MATERIAL APPEARING IN THIS THESIS (OTHER THAN BRIEF EXCERPTS REQUIRING ONLY PROPER ACKNOWLEDGEMENT IN SCHOLARLY WRITING) AND THAT ALL SUCH USE IS CLEARLY ACKNOWLEDGED.

TABLE OF CONTENTS

	Page
ABSTRACT	ii
TABLE OF FIGURES	iii
ACKNOWLEDGMENTS	iv
	Page
1.0 INTRODUCTION	1
1.1 Statement of Purpose	1
1.2 Methane and the environment	1
2.0 HOLCENE CLIMATE	3
2.1 Insolation	3
2.2 Laurentide Ice Sheet	4
2.3 Trace Gas Concentrations	5
2.4 Holocene Climate in the Arctic	5
3.0 PERMAFROST	10
3.1 Ground Ice	12
3.2 Thermokarst	15
3.3 Thaw Lakes	18
3.4 Geographic Distribution	21
3.4.1 Siberia	22
3.4.2 Alaska	23
3.4.3 Western Canadian Arctic: Yukon Coastal Plain	24
3.4.4 Western Canadian Arctic: Tuktoyaktuk Peninsula	25
4.0 THE MODEL-An Overview	26
4.1 Mass Movements	27
4.2 Thawing and Subsidence	31
4.3 Lake Ice	31
4.4 Initial Parameters	32
4.5 Site Specific Parameters	32
4.5.1 Taymyr Peninsula	33
4.5.2 Labaz Lake	35
4.6 Temperature Data	38
4.7 Methane Calculation	38
5.0 RESULTS	40
5.1 Radial Growth	40
5.2 Talik Growth	43
5.3 Methane	45
5.4 Sources of Error and Limitations	48
6.0 DISCUSSION	50
6.1 Radial Growth and Talik Depth	50
6.2 Methane Release	51
7.0 CONCLUSIONS AND FUTURE WORK	54
8.0 REFERENCES	56

TABLE OF FIGURES

Figure		Page
2.1	Map of northern North America	6
3.1	Map of Permafrost Zones in the Arctic	10
3.2	Schematic showing permafrost terminology	11
3.3	Schematic showing how ice wedges form	14
3.4	Picture of an ice wedge in Liverpool, Alaska	14
3.5	Aerial view of ice-wedge polygon network from the Beaufort Coastland, western Arctic coast, Canada	15
3.6	'Drunken trees' in a thermokarst landscape, Alaska	17
3.7	A thaw lake	18
3.8a	Slope margin of a thaw lake	19
3.8b	Perimeter of a thaw lake	19
3.9	Thaw lake landscape from the Tuktoyaktuk Peninsula, Canada	20
4.1	Location map of the Taymyr Peninsula	33
4.2	Location map for the Taymyr (Taimyr) Peninsula study site	34
4.3	Average paleoclimate curves for Taymyr sections pollen	35
4.4	Location map for the Arctic (A), Taymyr-Severnaya Zemlya Peninsula (B) and Labaz Lake (C)	36
4.5	Averaged paleoclimate curve from Labaz Lake sites pollen	37
5.1	Averaged paleoclimate curve from fossil pollen	42
5.2	Annual expansion rate (m)	42
5.3	Total lake radius expansion (m)	42
5.4	Talik deepening rate (m)	44
5.5	Talik depth (m)	44
5.6	Methane released (kg/yr)	47
5.7	Cumulative methane release (kg)	47
6.1	Natural and Anthropogenic Sources of Methane	53

ABSTRACT

Thaw lakes form as a result of disturbances to permafrost that cause differential thawing. Thawing at the lake margins causes slumping that expands the lake radially at rates dependent on substrate properties, such as excess ice content. The thaw bulb, or talik, descends beneath the lake, causing subsidence as thawed sediments regain their native porosity.

Thaw lake landscapes span approximately 1 million km^2 of Siberia, a region underlain by Pleistocene-age organic-rich peat, called yedoma. As thaw lakes expand, methanogensis converts carbon from the thawed permafrost into methane, a greenhouse gas. Recent studies have shown that thaw lakes are a larger source of methane in the atmosphere than previously believed, compared to other major natural sources.

Here I use Holocene climate reconstructions from the central and western part of the Taymyr Peninsula in northern Siberia to drive a thaw lake model simulation. The results show how small temperature differences between two localities can lead to large differences in thaw lake size and depth. The quantity of methane released from the lakes over the Holocene was used to calculate the quantity of methane released from Siberia over the Holocene, and also on a yearly basis. The results show that Siberian thaw lakes have contributed, and will continue to contribute methane at the regional, if not global scale; an important factor when considering positive feedback systems for current climate change.

ACKNOWLEDGMENTS

First and foremost I would like to thank Dr. Lawrence Plug for all his guidance and patience this year. I would also like to thank Dr. Patrick Ryall for his advice and keeping us on track and on time. Finally, this thesis would not have been possible without the constant support of family and friends, particularly all those in the Earth Science Department at Dalhousie University.

1.0 INTRODUCTION

1.1 Statement of Purpose

The purpose of this thesis is to model thaw lakes in two dimensions over the period of the Holocene (10 000 ka to present). The modelling was done using MatLab and built using a previous thaw lake model. It is of particular interest to observe the changes in lake morphology during periods of warming, such as the Holocene Thermal Maximum. By modelling lakes during periods of warming, I hope to be able to make some inferences about how lakes will respond to current warming conditions. I will also try to draw some conclusions regarding lake expansion and what effects, if any, this may have on climate feedback systems.

1.2 Methane and the Environment

Methane is more potent that carbon dioxide in the atmosphere as a greenhouse gas. Each molecule of CH_4 is twenty times more effective than one molecule of CO_2 at trapping infrared radiation, yet CO_2 is 200 times more abundant than CH_4 in the atmosphere, 1.7 ppmv (parts per million by volume) of CH_4 compared to 350 ppmv of CO_2 (EPA, 2006).

In northern Siberia there is an estimated 400 000 Tg (1 Tg = 10^{12} g) of Pleistocene aged organic carbon stored in frozen sediments [Zimov et al, 1997]. It is estimated that 5% of carbon released per m^2 from thawing is in the form of methane, or 65± 3 mg CH_4 g^{-1} sediment [Zimov et al, 1997]. Temperatures in the Arctic are rising faster than anywhere else in the world [Chapin et al, 2005]. Increased temperature would mean that more methane would be

released into the atmosphere as frozen sediments begin to melt, contributing to the cycle of global warming. What role thaw lakes play in releasing methane into the atmosphere is addressed in the following chapters.

2.0 HOLOCENCE CLIMATE

The Holocene is the geological period spanning the last 10 000 years. As it is the most recent of geological time periods climate records are generally accurate. Arctic North America has experienced a very dynamic Holocene climate, the most prominent feature being the Holocene Thermal Maximum (HTM). This was a period of wide scale warming whose onset began in Alaska around 11.3 ka and moved across to Labrador around 6ka. This period of warming was induced by two main forcings: summer insolation changes and the retreating Laurentide Ice Sheet (LIS) [Kaufman et al, 2004; Kaplan and Wolfe, 2006].

2.1 Insolation

Insolation, the radiation the earth receives from the sun, changes due to orbital scale dynamics [eg. Kutzback, 1981, and Kaufman et al, 2004]. At the beginning of the Holocene, summer insolation was 7.2% higher than present at 35°N and 7.5% higher at 70°N [Kutzbach, 1981]. Conversely, winter insolation was lower, by an average of 6% [Berger and Loutre, 1991]. This change in insolation was caused by: a higher obliquity (24.23° compared with present value of 23.45°), a summer perihelion (July 30th compared with the modern date of January 3rd) and a greater eccentricity (0.0193 compared with a modern value of 0.0167) [Kutzbach, 1981]. At high Arctic latitudes the lack of winter sunshine means that summer insolation quantities are much more important [Kaplan and Wolfe, 2006]. Though peak summer insolation occurred around 11-9ka, the HTM lags this by at least 1000 years [Kaplan and Wolfe,

2006] and in some cases several thousand years [Kaufman et al, 2004], reasons for which will be discussed shortly.

2.2 Laurentide Ice Sheet

At the beginning of the Holocene the Laurentide Ice Sheet was still a prominent feature in Canada, encompassing and area of 1.5×10^6 km^2 across the Foxe Basin and much of Quebec and Labrador [Kaplan and Wolfe, 2006]. Though the presence of this huge ice mass had a substantial effect on regional atmospheric and ocean circulation, there was a pronounced climate gradient, the closet proximities suffering from the greatest effects [eg. Kaplan and Wolfe, 2006].

Regions downwind of the LIS received more cold air through atmospheric advection as well as a cold water flux from meltwater and iceberg calving into nearby seas [Kaufman et al., 2004]. The Labrador Sea in particular was intensely cooled by the LIS, which had the effect of displacing the jet steam south [COHMAP, 1998; and CAPE, 2001]. Sea surface temperatures on the Labrador Shelf were suppressed until the Mid Holocene, as confirmed by high concentrations of cold freshwater benthic foraminifera [Kaufman et al, 2004]. The large freshwater influx also had the effect of disturbing formation of North Atlantic Deepwater [Licciardi et al, 1999; in Kaplan and Wolfe, 2006 and Clark et al, 2001], which had implications for global ocean circulation.

As the LIS was retreating during the Holocene, the reduced ice cover and increased vegetation lowered the surface albedo. This meant that more solar energy was stored in the summer than re-radiated in the winter [Gildor and

Tziperman, 2001 in Kaufman et al, 2004]. This was a positive feedback system for promoting the initiation of vegetation, such as the expansion of forests over tundra, after the removal of the glacier. The LIS disappeared completely by about 6ka [Kaplan and Wolfe, 2006].

2.3 Trace Gas Concentrations

Climatic records indicate that CO_2 levels reached pre-Industrial levels, 278 ppm, around 11ka and decreased to about 260 ppm though the early to the mid Holocene [Indermühle et al, 1999]. Methane levels decreased significantly during the early to middle Holocene, from 725 ppbv to 670 ppbv [Blunier et al., 1995]. This indicates that Holocene warming was not caused by increased greenhouse gases, but rather was solely the result of insolation increases. However, Holocene warming did likely cause the increase of water vapour content in the atmosphere and also increased in the flux of heat and moisture from the tropics [Kaufman et al., 2004]. Increased water vapour content is a positive feedback system, trapping atmospheric heat.

2.4 Holocene Climate in the Arctic

Though increased summer insolation is a uniform forcing at the same latitude, it did not create a uniform HTM either spatially or temporally [eg. Kaufman et al, 2004]. The presence of the LIS is the most obvious and likely factor in determining the distribution of the HTM. A variety of climate proxies are used to track the HTM across the North American Arctic. Proxies are physical, biological and chemical evidence from which age and temperature can be inferred. Some examples of proxies that are used are: pollen, plant

macrofossils, microfossils, treeline position, stable isotope composition, preserved organic rich layers such as peat, and lake pH.

Alaska (Location #1, Figure 2.1) shows the earliest onset of the HTM as it was the furthest from the LIS. Dated peat deposits show that HTM began around 12.9ka and reached a maximum from 9.7-9.2ka [Kaufman et al, 2004]. Beetle remains found beyond their modern northern limits were used to infer a warming of about 2-3° C in Alaska at about 10.8 ka [McCulloch and Hopkins 1966 from Kaufman et al., 2004]. This was verified by pollen and plant macrofossil evidence, indicating that the poplar (*Populus balsamiferal)* treeline was also much further north 10ka then it is currently [Hopkins et al 1981 from Kaufman et al. 2004].

Figure 2.1- Map of northern North America and the Atlantic (from University of of Texas Libraries www.lib.utexas.edu/maps/americas/canada_rel97.jpg)

The Yukon (Location #2 on Figure 2.1) showed a HTM around 10.6ka. This is inferred from the spruce genus *Picea* pollen and needles, indicating the treeline was up to 75km further north than present at the height of the HTM [Kaufman et al. 2004]. The *Picea* pollen also indicate that present day temperature levels were reached between 6.7 and 5.6ka [Kaufman et al., 2004].

The Tuktoyaktuk Peninsula (Location #3), in the Northwest Territories has several HTM climate proxies. Tree stump remains and *Picea* pollen indicate warming of about 3° C between 10.3ka and 9.1ka [Spear, 1993 in Kaufman et al., 2004]. Other evidence from the Peninsula includes: peak formation of thaw lakes between 11.6-10.3ka [Rampton, 1988 in Kaufman et al., 2004], thickening of the active layer in permafrost which is seen as a thaw unconformity dating to about 9ka along the Yukon coast [Burn, 1997], and increased peat development [Vardy et al., 1997].

The region east of the MacKenzie Mountains to Hudson Bay (Location #4) shows very convincing evidence of HTM. During the HTM The continuous permafrost line is believed to have shifted northward 300-500km. This is inferred from widescale peatland development in this region at that time [Zoltai, 1995 in Kaufman et al, 2004 and Vardy et al, 1997] though that region is again within the continuous permafrost zone.

Quebec and Labrador (Location #5) experienced the latest onset of the HTM, as the LIS was present here until at least 6.8ka. Southeastern Labrador began to warm around 8ka, which lasted until 6ka [Sawada et al, 1999 in

Kaufman et al., 2004]. The northern part of this region experienced the peak HTM as late as 3.7ka, which we know from *Picea* pollen gathered from the surrounding area [Gajewski and Garalla 1992, and Gajewski et al 1993].

An interesting proxy used to infer changes in sea-ice cover in northern waters is the recovery of marine mammal bones from the ocean floor. An abundance of bones in the far north indicates reduced ice cover and thus warmer temperatures, as there is less inhibiting northward migration. Studies in the Arctic Ocean (Location #6) have shown a pronounced abundance of both Atlantic and Pacific bowhead whalebones, much further north than present migration would take them, between 10.5-8.5 ka, indicating a longer ice-free season [Dyke et al, 1996 and Dyke and Savelle, 2001].

Lake-core taken from eastern Baffin Island (Location #7) records a pronounced warming between 10 200 to 8 500 calibrated years B.P. [Briner et al. 2006]. Chironomids (mosquito type insects), diatoms, percent total carbon and lake pH were all used to infer this warming. Chironomids also tell us about the peak summer temperature, which are inferred to be approximately 11° C [Briner et al. 2006]. The Early Holocene is thought to be between 2-4°C warmer than the Late Holocene, as seen from chironomid and $\delta^{18}O$ records [Woller at al, 2004 in Briner et al. 2006]. These same techniques indicate a sharp, followed by a gradual, cooling after the HTM. Average annual temperatures eventually level out to approximately 6°C [Briner et al. 2006].

Pollen data collected from another location on eastern Baffin Island (Location #8) indicate peak warming of +1°C warmer than present between

8.6ka and 5.7ka [Kaufman et al., 2004]. This later peak HTM within a rather small geographical area illustrates the necessity to be cautious when comparing different types of proxy data. Proxy data that record peak summer temperatures show earlier and greater Holocene warming because of more pronounced seasonality at the beginning of the Holocene [Berger and Loutre, 1991 in Briner et al., 2006]. Whereas proxies that record mean annual temperatures will not be as susceptible to seasonality variations, and will show more subtle warming later in the Holocene [Briner et al., 2006].

In summary, the warmest period in the Arctic occurred from 8.9 +/- 2.1ka to 5.9 +/-2.6ka. The large standard deviations represent the large spatial-temporal variations in the onset of HTM. Alaska showed the earliest warming, on average beginning 11.3 +/- 1.5ka, and lasting 2200 +/- 1300 years. This contrasts with northern continental Canada, which experienced HTM starting at 7.3 +/- 1.6 ka and lasting 3400 +/-1400 years. The spatial-temporal variations are attributed almost entirely to the presence of the decaying Laurentide Ice Sheet over northern continental Canada [Kaufman et al., 2004].

The terrestrial record shows an average temperature of 1.6°C +/- 0.8°C warmer than present during the HTM. The marine record shows a more pronounced warming of 3.8 +/- 1.9°C at HTM peak compared to present average temperatures for the same region. It is interesting to note that the average maximum temperature of the HTM is the same, regardless of time or place within the Arctic region [Kaufman et al., 2004].

3.0 PERMAFROST

Permafrost is a widespread phenomenon, existing beneath 1/5 of the world's land surface and beneath 22% of the continental northern hemisphere (Figure 3.1) [Davis, 2001]. Permafrost is a term used to describe ground that has been consecutively frozen for 2 or more years. Cryotic ground is synonymous with permafrost but it refers only to the temperature state (< 0°) and not the water or ice content of the ground [French, 1996]. Frozen ground however, implies there is water within the ground and it is in the form of ice [French, 1996].

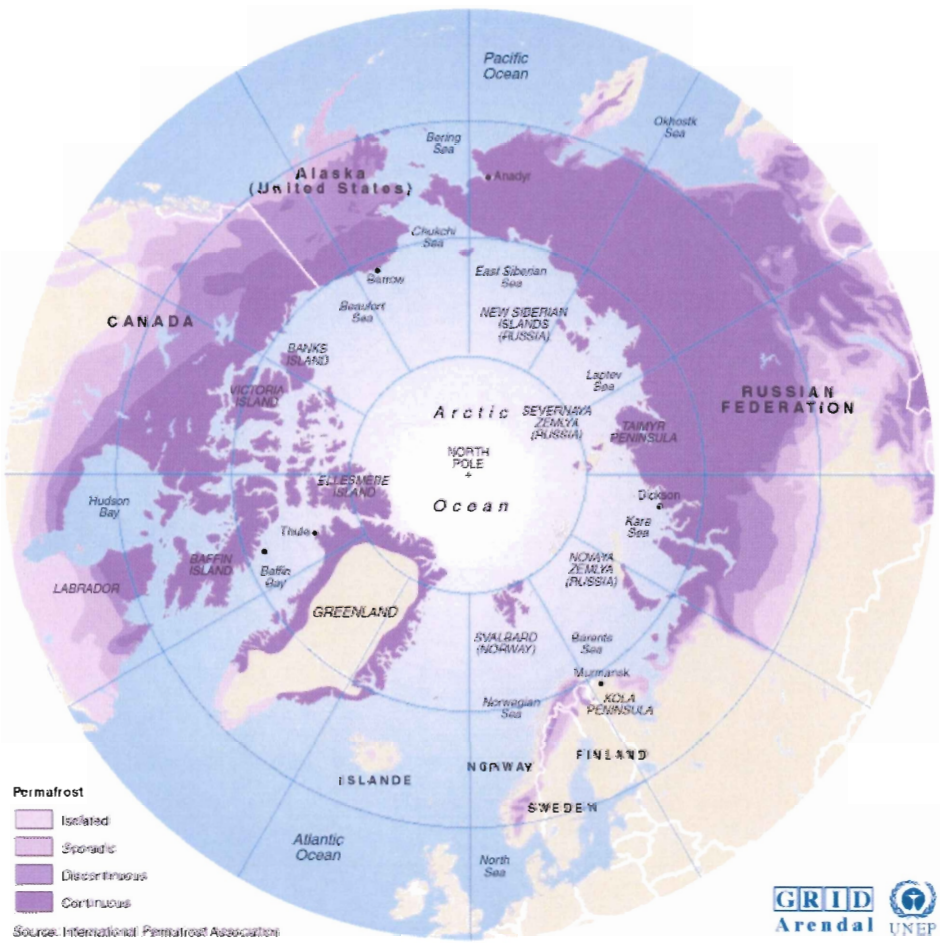

Figure 3.1- Map of Permafrost Zones in the Arctic (from International Permafrost Association)

Figure 3.2 illustrates some of the permafrost terminology. The active layer refers to the top layer of the ground surface that annually freezes and thaws. The permafrost table is the top of the permafrost zone, usually the bottom of the active layer. Unfrozen zones can exist between the active layer and permafrost table, called *taliks*. Taliks also can exist as pockets within permafrost or beneath bodies of water, such as thaw lakes. Continuous permafrost contains permafrost everywhere beneath the ground. It can contain taliks within the permafrost layer or below bodies of water. Discontinuous permafrost refers ground that is not completely covered by permafrost but rather contains pockets of unfrozen ground that pierce the active layer.

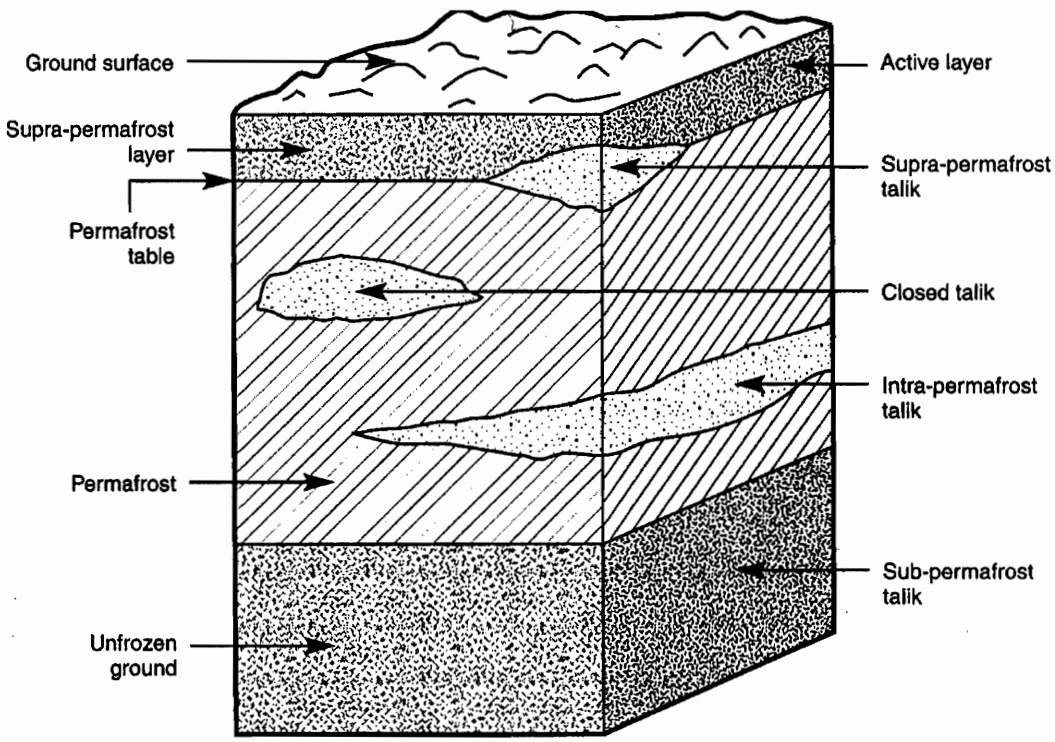

Figure 3.2- Schematic showing permafrost terminology (from French, 1996)

The depth of permafrost is determined by: mean annual temperature, geothermal heat flux, proximity to standing water, past climate and climatic stability [French, 1996]. By multiplying the absolute value of a mean annual temperature of -10°C by a typical geothermal gradient of 1°C per 50m we can expect a permafrost thickness of 500m [French, 1996]. As this equation is only an average, other factors mentioned must be considered. Standing water will raise the surface temperature, and past climate change can create produce a thickness of permafrost not related to present conditions. For example, thick permafrost can exist even in places where it is currently warm, because in the past the climate was colder. In Canada, permafrost thicknesses can range between a few tens of meters in northern Manitoba to 400m in the Northwest Territories [Brown, 1970]. The greatest depth of permafrost recorded is 1450m in Siberia [Grave 1956 in Washburn 1980].

When water freezes it expands by 9%. However, water-saturated soils can expand between 50-100%, even more if fine-grained sediments exist with an underlying water source. This expansion factor is very important as thawing can create significant subsidence, plaguing construction efforts in northern regions [Davis, 2001].

3.1 Ground-ice

Ground-ice refers to any type of ice that forms in the cavities and voids within soil and sediment that freezes. It typically dominates the top 1-3 meters of the permafrost zone in arctic North America. Ground with less than 40-50% ice content is considered to have a low ice-content, whereas anything

between 50-150% is considered to have a high ice content [French, 1996]. The highest ice content usually occurs in fine grained sediments. Ice content in excess of porosity (greater than 100%) is called excess ice [French, 1996].

Pore ice forms from water that is already present within the soil when is freezes. It is most typical of the ice types below depths of 10m within permafrost. It can force soil particles apart, squeezing and altering them [Davis, 2001].

Ice wedges form when permafrost cracks due to thermal contraction during mid-winter cooling, relieving tensile strength in the direction perpendicular to the maximum stress [Lachenbruch, 1962]. Water accumulates in the cracks during the summer thaw, then freezes in the winter. The ice is more susceptible to cracking during subsequent winters because it is weaker than the surrounding soil. The process of ice-crack formation is illustrated in Figure 3.3. Ice-wedges are typically 1-1.5m wide at the surface and 3-4m deep, as seen in Figure 3.4. In Siberia ice-wedges up to 4-5m wide and 5-10m deep have been recorded [French, 1996].

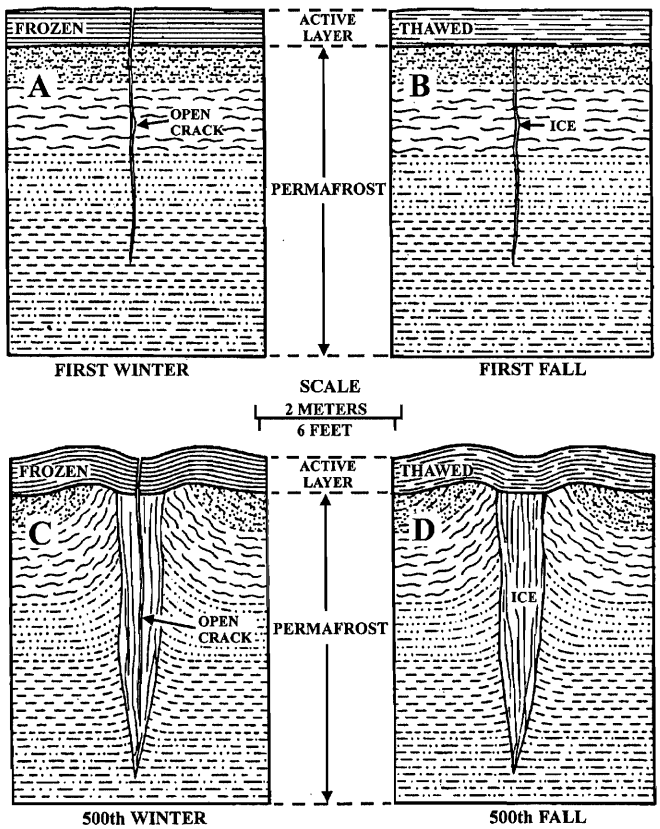

Figure 3.3- Schematic showing how ice wedges form (from Lachenbruch, 1962)

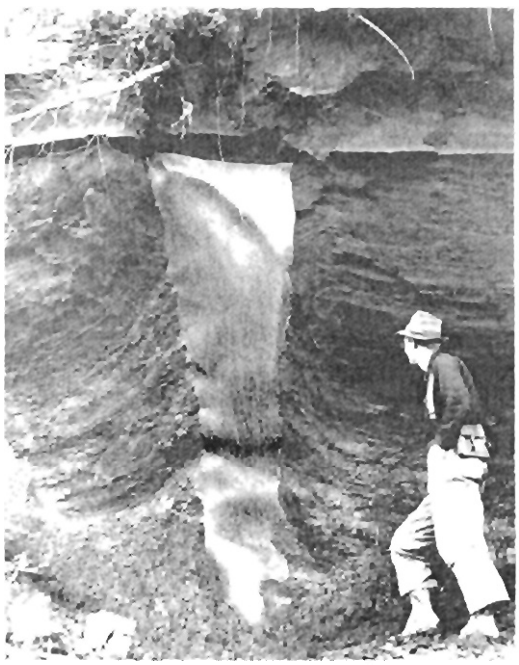

Figure 3.4- Picture of an ice wedge in Liverpool, Alaska (photo from Troy L. Pewe 1949 from Davis, 2001)

In plan view ice wedges commonly form polygons (Figure 3.5). These polygons are 15-40m across and most intersections are orthogonal. Polygons may be either strongly oriented (typically found around water bodies) or randomly oriented [Lachenbruch 1962, 1966].

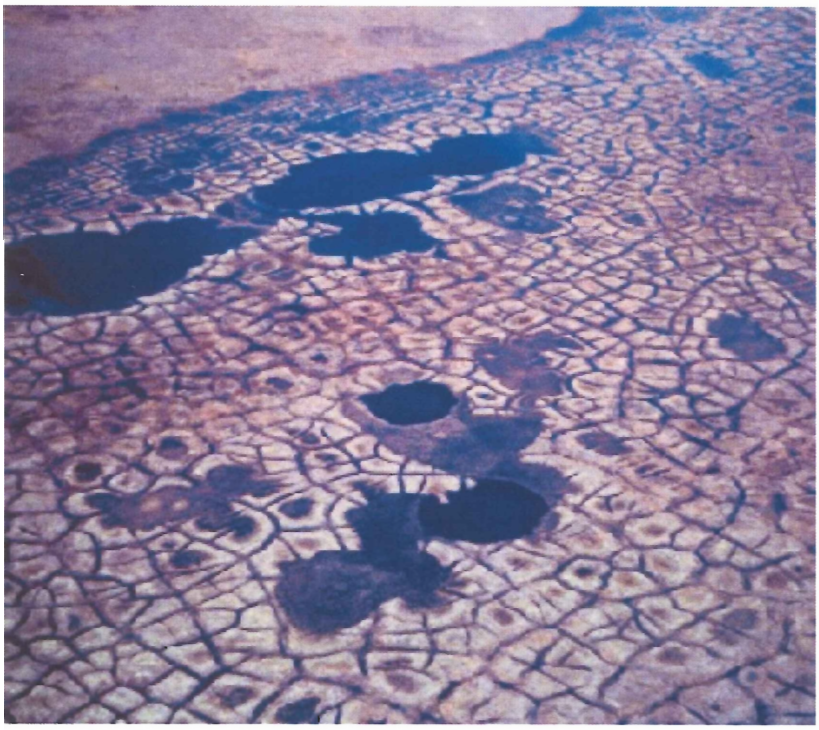

Figure 3.5- Aerial view of ice-wedge polygon network from the Beaufort Coastland, western Arctic coast, Canada (from Natural Resources Canada)

3.2 Thermokarst

Thermokarst landscape develops when permafrost that contains excess ice begins to thaw [French, 1996]. This can be caused by climate warming or by disruptions of the surface that cause the active layer to expand downwards locally. Subsidence and compaction of the ground, particularly where large quantities of ice-rich permafrost exist, occur as melting progresses. Once subsidence begins and depressions form, the area around the depressions will

become unstable and begin to slump as well [Williams and Smith, 1989]. The relief formed from the melting of permafrost is directly related to the amount and distribution of the excess ice as well as the thickness of permafrost thawed.

Flowing water is a common trigger for melting permafrost, as the conductive-convective process of flowing water on frozen sediment allows thawing to begin [Williams and Smith, 1989]. Once initiated, soil movement and vegetation loss continue the melting process. The most dominant physical process is the slumping of thawing ground, exposing frozen ground and allowing it in turn to begin the thawing process [Williams and Smith, 1989].

Standing water also can create thermokarst, particularly when coupled with ice wedge polygons. Water can accumulate in the centre of polygons, at the junction of two ice wedge cracks or even in the trough above individual cracks. These bodies of water then allow more melting of permafrost in the summer and less freezing in the winter, deepening the depressions, allowing more water to accumulate [French, 1996].

Disruption and/or removal of vegetation is another way to quickly initiate melting of permafrost. This is because vegetation acts as insulation over the grounds surface, preventing the melting of permafrost even when the climate warms [Davis 1996]. The removal of vegetation can be a natural occurrence or the result of anthropogenic activity such as clearing of land for foundations or vehicle traffic.

Forest fires in boreal regions can quickly increase the depth of the active layer between 40-100% only a few years after the fire [French, 1996]. However, the long-term effects of the fire greatly depend on the regional permafrost conditions and climate.

The result of thawing of permafrost is an undulating landscape, with sinks, depressions and mounded topographic highs. 'Drunken trees' are an interesting feature of a thermokarst landscape, illustrated in Figure 3.6. This happens when the permafrost in which trees are rooted in (often around the perimeter of a thermokarst lake) thaws, and the trees begin to tilt haphazardly in various directions.

Figure 3.6- 'Drunken trees' in a thermokarst landscape, Alaska (from Davis, 2001)

3.3 Thaw Lakes

Bodies of water that result from the melting of ice-rich permafrost are called thaw lakes. Figure 3.7 is a typical thaw lake. They typically occur in flat low-land areas where there are thick deposits of silty, clay alluvium [Burn and Smith, 1988]. Thawing is initiated when climate begins to warm or if a larger temperature amplitude begins to develop, which increases the freeze-thaw process. Localized initiation can result from the disruption of the thermal equilibrium of the active layer, such as when vegetation is disturbed. Once water begins to accumulate it conducts heat to the frozen ground and allows it to begin to thaw [Hopkins, 1949].

Figure 3.7- A thaw lake (Courtesy of L.J. Plug)

Thawing occurs most rapidly at water level, where thawed ground extends tens of centimeters into the bank. Slumping and undercutting are the main contributors to radial expansion of the lakes. As lakes grow, wind and wave action erode the perimeter of the lake causing slumping and mass movements. This redistributes sediment along the lake bottom. Redistribution

allows fresh surfaces of frozen sediment to be exposed and to begin thawing [Hopkins, 1949]. Figures 3.8a and b shows what the perimeter of a thaw lake looks like.

Figures 3.8a and b-Slope margin and perimeter of a thaw lake (Courtesy of L.J. Plug)

Thaw lakes deepen as thawed ground compacts and subsides. Lakes will continue to grow until they expand vertically through the ice rich zone of permafrost, which can take thousands of years, or they can drain very rapidly (order of hours to days) if the lakes encounter a topographic low when they expand [Brewer *et al*, 1993 in West and Plug, *accepted*]. Lake depths are

variable, for example, 1-4m in parts of Siberia [Tomirdario, 1982] and 0.3-1.8m for Holocene Lakes on the Seaward Peninsula of Alaska [Hopkins, 1949], and up to 20m deep in thick ice-rich Pleistocene loess.

Thaw lakes characteristically have steep sides and a flat bottom. Some lakes have littoral terraces that can range from 100m to 1km from shore [West and Plug, *accepted*], though how these shelves form is still controversial. The bathymetry of lakes depends on lake age, lake radial expansion, and the thickness of the layer of ice-rich permafrost [West and Plug, *accepted*]. The last factor is dependant on how and under what conditions the sediments were deposited, as well as whether the current thaw lake is in virgin ice or if it formed in the basin of a previous thaw lake [West and Plug, *accepted*]. Older lake basins put constraints on the dimensions of subsequent lakes that form. Lakes are larger, deeper and rounder if they form in deep, ice-rich, virgin permafrost. Figure 3.9 is aerial view of the Tuktoyaktuk Peninsula, showing many generations of thaw lakes, some overlapping.

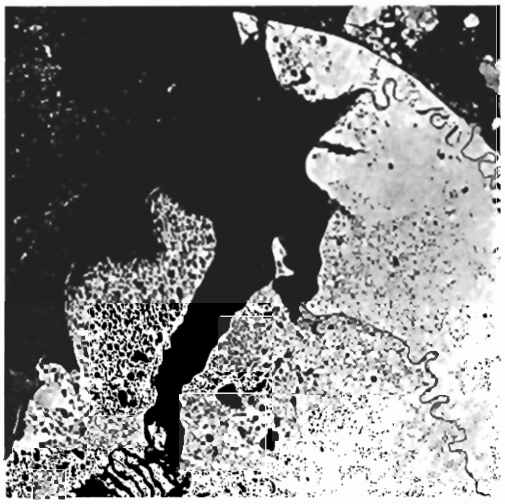

Figure 3.9- Thaw lake landscape from the Tuktoyaktuk Peninsula, Canada (from Landsat)

Lake expansion rates are highly variable and also depend on the characteristics of the permafrost. A few tens of centimetres up to a meter per year of expansion are typical of the central Yukon and the Northern Seward Peninsula of Alaska [Rampton, 1988]. However, expansion rates as high as 4.5 m/yr on the Tuktoyaktuk Peninsula [Rampton, 1988] are recorded and 10 m/yr has been recorded for Siberia [Tomirdiaro, 1982], though rates of 0-1m/yr are more common [Zimov et al, 1997 and Walters et al, 2005]

Oriented thaw lakes have been observed in many Arctic terranes, most notably Point Barrow Alaska [Carson and Hussey, 1962]. These lakes are not oriented parallel to the prevailing wind direction, as one might suppose, but in fact oriented perpendicular to it. This is another feature of thaw lakes not well understood. It is thought that prevailing winds move sediment and vegetation along the winds path to the far end of the lake where it is deposited [Carson and Hussey, 1962]. This creates an insulating mat that prevents thawing of the underlying permafrost. Subsurface water currents caused by the wind end up flowing faster along perpendicular edges of the lake. A 32 km/hr wind can cause subsurface currents up to 1km/hr at the cross-wind points of the lake. This is strong enough to move sand and small gravel 100m/hr along the shore [Davis, 2001].

3.4 Geographic Distribution of Thaw Lakes

Thaw lakes are not ubiquitous across all arctic regions. There are a few specific regions in which they do occur and each has its own characteristics. Siberia, the Northern Alaska Coastal Plain and the Western Canadian Arctic

contain the most common occurrences of thaw lakes. Each shall be discussed in turn in the following section.

3.4.1 Siberia

Central Yakutia in eastern Siberia is often considered the type locality for thermokarst and thaw lake development, though the circumstances under which the environment developed are quite unique [French, 1996]. During the Quaternary, Central Yakutia remained completely ice free, or nearly so. This allowed thick deposits of fine-grained alluvium to accumulate. This silty loam now contains between 50-80% segregated ice lenses and large (50-60m deep) ice wedges. Not only is permafrost ice-rich but it is also very organic rich, containing about 2% carbon by weight [Walter, *et al*, 2006].

Permafrost here can reach a thickness of 600m [Schwamborn *et al*, 2002]. This region experiences one of the largest seasonal temperature amplitudes in the world, with a 62°C between the height of summer and the coldest winter day [French, 1996]. This extreme temperature range has led to the development of a 2m thick active layer. Within the continuous permafrost zone in Siberia there is an area of 1 million km^2 of thaw lakes both active and drained [Zimov et al, 1997 and Walters et al, 2005].

Because of both the extent and organic content of the thaw lake region many scientists are concerned about this region becoming warmer [eg Walter *et al*, 2006]. As the organic-rich permafrost melts from expanding thaw lakes, it releases methane. It is estimated that every spring after the ice covering the thaw lakes melts 1-3.4 Tg of methane is released [Plug and West,

accepted]. In northern Siberia the rate of methane released is estimated at 3.7 Tg per year, based on bubble-flux measurements from selected lakes [Walter *et al,* 2006]. This volume is large enough to cause a spike in atmospheric concentrations of methane every spring thaw [Zimov et al, 1997]. As methane is a more potent greenhouse gas than carbon dioxide there are concerns that it could be a positive feedback system for climate change. Warming temperatures mean thaw lakes expand, releasing methane which in turn warms the atmosphere further causing the release of more methane. In a study done by Walter *et al* [2006] comparing lakes in northern Siberia between 1974 and 2000 a 14.7% increase in the area of thaw lakes was found, which equals a 58% increase in methane from this region over this time. Plug and West [*accepted*] predict an increase of 3-4 times the current volume of methane released per year within 200 years for a rate of 0.3°C/decade, owning to a faster radial expansion and larger lakes. These alarming projections make it vital to understand the process of thaw lake expansion under warming conditions.

3.4.2 Alaska

Thaw lakes occupy between 15-40% of the Northern Alaska Coastal Plain and drained lake basins occupy another 10-30% of the landscape [Hinkle *et al,* 2005]. Permafrost occurs to a depth of 300-600 m and the ground contains greater than 20% ice by volume in the top 10-20 m. Multiple glaciations accompanied by fluctuating sea level over the last 175 ky resulted in deposition of marine silts and sands, aeolian sands, alluvium and beach deposits [Hinkle *et al,* 2005]; this creates some spatial heterogeneity to thaw lake morphology.

The Seward Peninsula (western Alaska) has permafrost up to 100 m deep and excess ice comprises up to 80% of the substrate in the form of pore ice, lenses and wedges [Hopkins, 1949]. Thaw lakes occur in thick aeolian silt that was deposited during the Last Glacial Maximum when sea-level was at a lowstand [Goetcheus and Birks, 2001]. The active layer is approximately 1m and the talik beneath thaw lakes can reach almost 58m [Brewer *et al,* 1993 in Plug and West, *In Review*]. The Mean Annual Air Temperature (MAAT) is about -6°C [Plug and West, *In Review*] and this region does not experience the severe temperature amplitude of Siberia [French, 1996].

First generation thaw lakes that form in this region generally have a flat central basin with inclined margins toward the shoreline. This is thought to be characteristic of thaw lakes that form in deep ground-ice [West and Plug, *In Review*]. Lakes are also rounder and have smoother perimeters than lakes in shallow ground-ice or are later generation lakes.

3.4.3 Western Canadian Arctic: Yukon Coastal Plain

Glacial deposits including silts and sands of eskers, sands and clays from melt water channels and silts, and sands and clays from marine transgressions form the current Yukon Coastal Plain (YCP) along the Beaufort Sea [Rampton, 1982]. These units, up to 60m thick, were deposited between 130-74 ky ago during multiple advances and retreats of glaciers. Excess ice is found predominately in the top 1-3 m of fine-grained estuarine and colluvium deposits, and is approximately 60% of the substrate [Rampton, 1982].

In shallow ground-ice environments, thaw lakes quickly reach their maximum depth and spread out. This is the case with lakes found on the YCP and they have flat, uniform bottoms with steep margins [West and Plug, *In Review*]. Generally lakes found here are less than 4m deep, are more elliptical and have irregular perimeters [West and Plug, *In Review*].

3.4.4 Western Canadian Arctic: Tuktoyaktuk Peninsula

The Tuktoyaktuk Peninsula in the north-western Yukon is a poorly drained lowland area comprised of unconsolidated fluvial and marine deposits that were laid down during the Pleistocene [Rampton, 1988]. Permafrost is between 200m and 600m on the Peninsula and excess ground ice is concentrated near the surface [Burn, 2002]. Environment Canada data show that currently the Tuktoyaktuk Peninsula is undergoing the largest temperature increase of any place in Canada, 1.7° C increase in the last 100 years [Scott and Plug, in review]. The MAAT is now -9° C for the Tuktoyaktuk Peninsula [Scott and Plug, in review].

There are an estimated 10 000 thaw lakes on the Tuktoyaktuk Peninsula, covering at least 15% of the surface [Burn, 2002]. Many of the lakes have littoral terraces which can extend 100m from the shore and are generally 1m deep or less, meaning they freeze completely during the winter. Lakes found on Richard Island, just north of Tuktoyaktuk, have a modal diameter of 200m [Burn, 2002]. Because of the shallow ground ice, most lakes are 4m deep or less, though a few lakes as deep as 13m have been recorded [Burn, 2002].

4.0 THE MODEL- An Overview

The computer model, which I used to model the dynamics of a thaw lake during the Holocene, is described in West and Plug (accepted) and Plug and West (accepted). Here I summarize the model.

The model is a two-dimensional cross-sectional representation of a thaw lake. We model half of the lake (assuming lake symmetry), as we are more interested in the growth of the lake as opposed to the initiation of lakes. The model is composed of a grid of cells, each cell representing volumes of air, water, frozen ground or thawed ground. As well as phase, ground cells also have volumetric ice content. Heat capacity and thermal conductivity of the ground cells is dependent on the parameters of phase and ice volume content.

The upper boundary is air cells, whose specified temperature varies with time. These specified temperatures are gathered from historical climate records. The lower boundary is deep within the ground and has an applied geothermal heat flux, based on conditions from the area in question. The right vertical boundary has no flux because it has geometric symmetry, representing the other half of the lake. The left vertical boundary also has no flux because it is taken to be an infinite surface.

The initial ice content of the frozen ground is decided based on conditions from the study site. Naturally, however, the ground ice has a heterogeneous distribution due to ice wedges, lenses and veins. This in turn affects the thermal diffusivity. In the model, this heterogeneity is dealt with by imposing a normal-distributed variability in the mean ground ice content.

The mean ice content decreases linearly with depth until it reaches a value equal to the native porosity of the soil. The ground that is not ice is a homogenous unconsolidated soil that is distributed with spatial uniformity in the model.

The time step in the model is one day; that is, in each day of the model the morphology will change because of thawing, thaw subsidence, mass movement of the slopes and redeposition of sediment along the lake bottom. Each of these processes shall be discussed in the following sections.

4.1 Mass Movements

There are two types of mass movements that are dealt with in the model: relatively rapid processes (including slope failures, debris flows, mud slides) and slow constant processes (such as creep). The rapid processes can transport material from the slopes into the lake basin from meters to hundreds of meters, sometimes as turbidity currents. Though these momentum driven processes are rapid they are only episodic. This is opposed to the second type of mass movement that the model deals with, creep. This slow but constant process is caused by freeze-thaw cycles which are associated with expansion and contraction, as well as other small disturbances caused by vegetation and rainsplash. Creep is modelled as a linear diffusion process, which works well for a broad spectrum of climates and ground types [Roering et al, 2001].

Another process that transports material from lake margins to middle of the lake is rafting. This occurs when the ground is particularly ice rich and blocks of peat and frozen ground detach from the lake margins and float (raft)

on the surface of the lake until thawed or waterlogged. Though this process is not constant or frequent it has the potential to carry large amounts of debris far from the lake margins. Rafting, however, is not dealt with directly in the model. Instead it is incorporated into the probability that the distance material will travel form the margins. This will be discussed further.

The standard equation used to treat non-linear sediment transport is:

$$q = \frac{K\Delta z}{1-(\Delta z/S_c)^2} \qquad (1)$$

Where **q** is the sediment flux, **z** is the elevation above a datum, $\mathbf{S_c}$ is the critical slope angle for the material and **K** is a rate constant.

This equation incorporates both creep and advective processes; when z << S_c then the equation approaches $q=K\Delta z$ and we have creep. As Δz increases the sediment flux rapidly increases, approximating mass movements which do not travel great distances. There are a few limitations to this equation and the one that is most pertinent is the treatment of long-range transportation. Rafting, rolling and toppling can transport material over one or more topographic depressions, whereas in this equation sediment must be deposited in the first depression before further transport can occur.

In the thaw lake model, the standard non-linear transport equation is treated slightly differently:

$$P_{E,i} = \frac{C_E S_i}{1-(S_i/S_c)} \qquad (2)$$

Where $\mathbf{P_{E,i}}$ is the probability of slope failure, $\mathbf{S_i}$ is the local slope, $\mathbf{S_c}$ is the critical slope angle, and $\mathbf{C_E}$ is a rate constant.

Material from position *i* on the ground surface has a nonlinear dependence on S_i, similar to (1). The S_c for thawed sediments is set to 45° [from Roering et al, 1999 and Howard, 1997], and to 90° for frozen sediments as frozen sediment can remain vertical for a short duration [West and Plug, 2006]. C_E is a rate constant, similar to (1), and incorporates the substrate properties of pore pressure, angle of internal friction and density as the overall property of shear strength. This means that a higher C_E represents a weaker soil. A value of 5×10^{-10} m^2 s^{-1} is chosen by running several simulations and comparing the results to actual measurements taken from study sites [West and Plug, 2006].

The shear strength of a potential failure plane beneath a soil column at a depth *h* is:

$$h\tan\Phi\cos\Theta^2(\rho-\rho_{water}), \qquad (3)$$

where Θ is the slope angle, Φ is the angle of internal friction and ρ is the density of the soil. Pore pressure reduces the shear strength, and pore pressure is also proportional to the density contrast of soil and water, as treated in equation (2). This is also what determines the value assigned to C_E.

As C_E increases bank retreat generally increases also, as C_E will determine how much sediment will detach in each time step. The relationship is not linear, as sediment can build up at the base of a slope and effectively

insulate it and prevent it from being thawed, thus retarding bank retreat to some degree.

After material from the bank at position *i* is detached and moves down slope, to the site of deposited (*k*) is governed by the probability function:

$$P_{D,k} = \frac{\Delta y_{i,k}}{(\Delta x_{i,k})^n} \qquad (4)$$

Where $\mathbf{\Delta x_{i,k}}$ is the horizontal distance between *i* and *k*, $\mathbf{\Delta y_{i,k}}$ is the vertical distance between *i* and *k*, and the exponent **n** is a dissipative function. The exponent *n* effectively sets the transport distance of the sediment, as the flow will lose energy as a function of distance. This exponent is the same for both subaerial and subaqueous transportation. As one would intuitively expect, the high density of water should increase the amount of dissipation per distance travelled. However, because water is denser than air it can hold particles in suspension and can also allow rafting of frozen blocks of peat. Both processes counteract the dissipative effects of water. West and Plug [accepted] quantified this in several sensitivity tests and establish a value of *n*=2.

The rate of deposition at a position *k* in our model is dependent on the radius of the lake and the distance of *k* from the centre of the lake as defined by the following equation:

$$D_{kt} = [1 + (r_{lt} - r_{k/}\ r_{lt})] \qquad (5)$$

Where $\mathbf{D_{kt}}$ is the rate of deposition at position *k* during the time step, $\mathbf{r_{lt}}$ is the radius of the lake, $\mathbf{r_k}$ distance from *k* to the centre of the lake.

4.2 Thawing and subsidence

Temperatures are updated daily in the model using a two-dimensional heat equation which is solved using finite difference schemes.

The phase change envelope is between -1° C to 0° C, typical for fine grained soils. The thaw front can only move through one layer of cells at a time.

Ground cells are assigned a thermal diffusivity (α) which is equal to thermal conductivity (k) divided by the heat capacity (c), which in turn is dependent on the whether the cell is frozen or thawed and also the ice or water content.

One of the most important characteristics of ice rich permafrost is that its porosity is in excess of the porosity it would have with no ice present. This means that as ice rich permafrost melts it compacts until it reaches its "native" porosity. In the model, a cell with 10% excess ice has a 10% probability of being removed from the model when it thaws. If a cell is removed, then the cells above it will shift down, simulating the subsidence process. Cells have a chance to be thawed at the lake margins and also the boundary between the talik (thaw bulb) and the underlying permafrost.

4.3 Lake Ice

In the model lake ice starts to form when the mean daily temperature is less than -1° C. The ice thickness increases linearly as the winter progresses, reaching a maximum just prior to the spring thaw. Once the mean daily temperature is >0° C then the ice thickness returns to zero. The exact ice

thickness is not important for lake dynamics, but rather it is included for completeness sake. More important however, is the fact that lake margins will not thaw while lake ice is present, and thus the lake will not expand.

4.4 Initial Parameters

The lattice used is 2000m horizontal×200m vertical with a cell size of 0.3×0.3m.

The initial radius of the lake was set to 5 m across, 3m deep with a bank slope of 60°, consistent with the size of a surface disturbance caused by a melting ice wedge- a common cause of thaw lake initiation. The shape of this disturbance is unimportant to our results however, because lakes will reach dynamic equilibrium within a few hundred years, regardless of the initial parameters [Plug and West, accepted], and so shape is unimportant to lake dynamics over thousands of years; the time scale that we address in the current study.

Ground ice was initially set at a maximum value of 80% at the permafrost table and decreases to the value of the porosity at a depth of 80m [West and Plug, accepted].

4.5 Site Specific Parameters

There are two locations in Siberia which have been chosen to be modelled over the Holocene. They are not in the type locality for thaw lakes however, but continuous temperature recreations spanning the Holocene exist for these localities. Equally important is the fact that thaw lakes in northern Siberia are underlain by a particularly organic-rich layer, called a yedoma,

which contains ~2% carbon by mass [Walter, 2006]; an important factor when considering methane release. Not every parameter was recorded for each site, so some educated guesses were made based on information from nearby sites with similar characteristics. I outline the site-specific parameters in the following sections.

4.5.1 Taymyr Peninsula

The Peninsula is located in northern Siberia between the Kara and Laptev Seas, Figure 4.1, and the study site is located on the western part of the Peninsula (Location #6 on Figure 4.2, 72°00´N, 96° 20´E). The Taymyr Peninsula is classified as modern tundra and tundra shrub zoned [Andreev et al, 2000]. The average July temperature is 4-6° C, compared with -32 to -34° C in January. The average annual precipitation is 250mm.

Figure 4.1- Location map of the Taymyr Peninsula (from Norman Einstien, 2005)

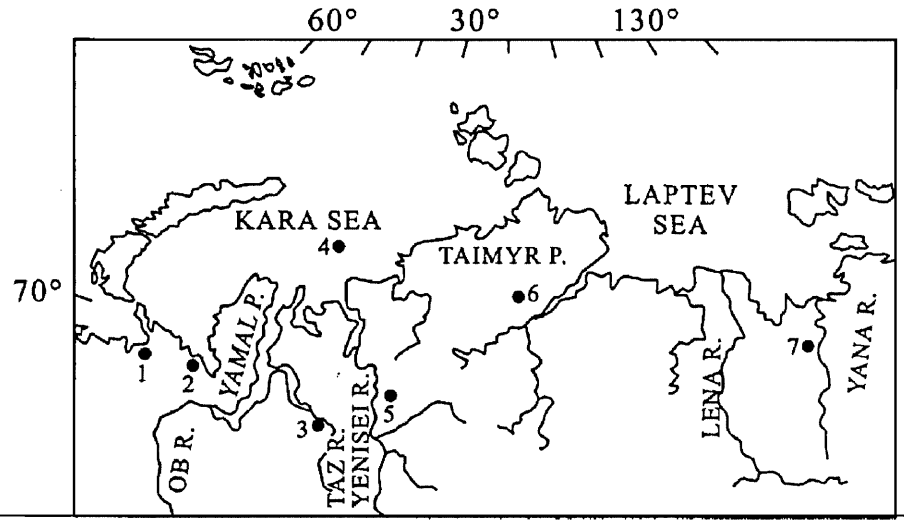

Figure 4.2- Location map for the Taymyr (Taimyr) Peninsula study site (from Andreev et al 2000).

Climate data for the Taymyr Peninsula was gathered from Andreev et al [2000] who reconstructed temperature records from fossil pollen. This was done by correlating fossil pollen assemblages found in drill core sections to modern pollen assemblages with known particular climates using a statistical-information method (transfer function). Bulk carbon-14 dates are used as chronological control on the core sections, which are all drilled in peat. The sampling interval reveals a time resolution of about 100 years. Statistical error for annual temperature is ± 0.6 °, ±1°C for July and January temperatures respectively [Andreev et al., 2000].

The Andreev et al. [2000] record is based on six sections sampled in the central part of the peninsula. The averaged paleoclimate curve extends back to 11 000 years before present, illustrated in Figure 4.3. Two anomalously warm and moist times are revealed by the reconstruction. One at about 8500 years BP, with T_{VII} (July temperature) almost 4° C warmer than present, T_I

(January temperature) 2.5° C warmer and annual precipitation values 100mm more than present. The second time is between 6000-4500 years BP where T_{VII} are 3°C warmer, T_I is up to 2° C warmer and at least 100mm more precipitation.

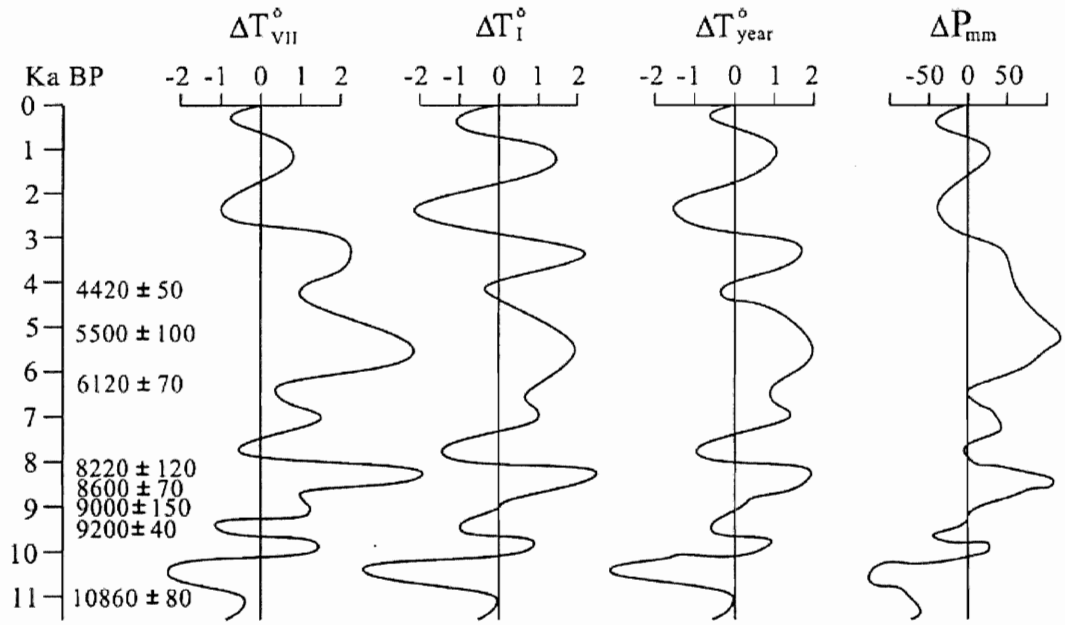

Figure 4.3- Average paleoclimate curves for Taymyr sections pollen (from Andreev et al 2000)

4.5.2 Labaz Lake

Labaz Lake is located on the Taymyr Peninsula at 68°51′N, 66°54′E (Figure 4.4), at the transition zone between the marine-influenced area West Siberia and continental influences of East Siberia and it characterized as typical Tundra. The location on Labaz Lake in this transition zone makes it particularly sensitive to climate change. The average temperature of the 8 month long winter is -32° to -34° C and summer temperatures are between 10-

12° C on average. The average annual precipitation is 300 mm. Permafrost thickness ranges from 300-600 m in the region.

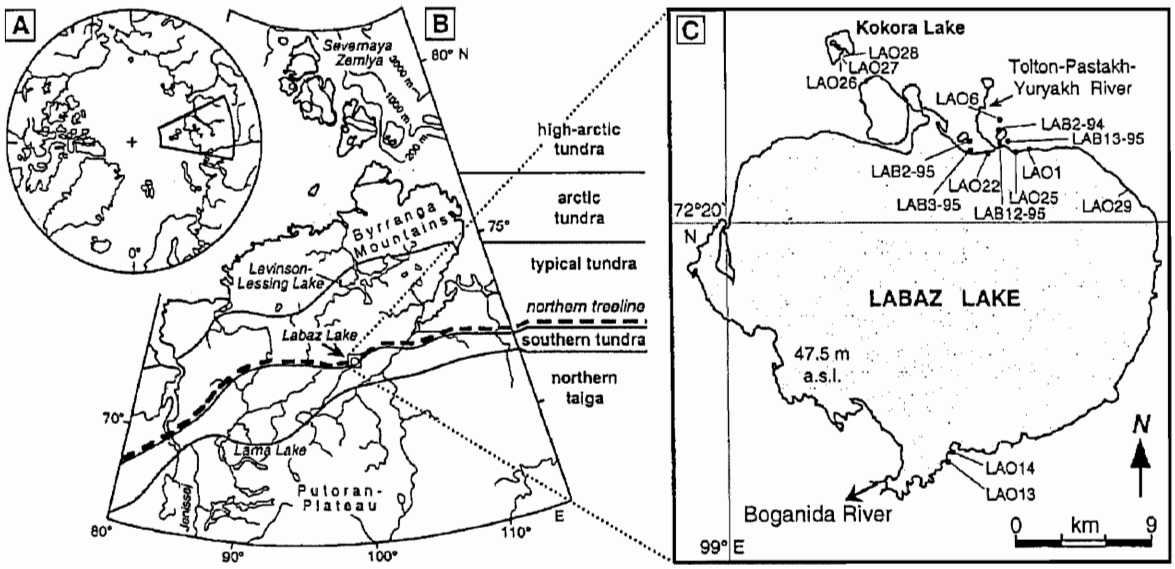

Figure 4.4- Location map for the Arctic (A), Taymyr-Severnaya Zemlya Peninsula (B) and Labaz Lake (C) (from Andreev et al 2002).

Climate data for Labaz Lake was compiled by Andreev et al. [2002] from fossil pollen spectra. 175 samples were collected for pollen analysis. Pollen percentages were calculated based on the total pollen sum. Percentages of spores were calculated using the combined total pollen and spore count.

A statistical method was used to correlate fossil pollen spectra (percentages of pollen and spores) to modern assemblages, based on 800 recent pollen spectra taken across the former USSR [Andreev et al, 2002]. The statistical relationship established between modern and fossil pollen assemblages is used to reconstruct past climates. Because the method is based on the use of arboreal (tree) pollen it works best when comparing fossil pollen spectra that are dominated by arboreal pollen. Fortunately the Holocene is

dominated by arboreal pollen, so we can conclude that the reconstructed climates are as accurate as possible within the constraints of the method. Some error does exist of course, annual temperature are accurate within ±0.6° C for, and July and January temperatures are accurate within ±1° C. About 40 samples were carbon-14 dated and used as chronological control.

Figure 4.5 is the graphical reconstruction of Holocene temperatures for Labaz Lake. The warmest time during the Holocene at Labaz Lake was between 6000-4500 ^{14}C years BP. Temperatures were between 2.5-3° C warmer than present and precipitation was 100mm greater. The coldest times were at 10 500, 4500 and 2500 ^{14}C years BP where temperatures were between 2.5 to 3° C colder than present. Precipitation was as much as 100 mm less than current.

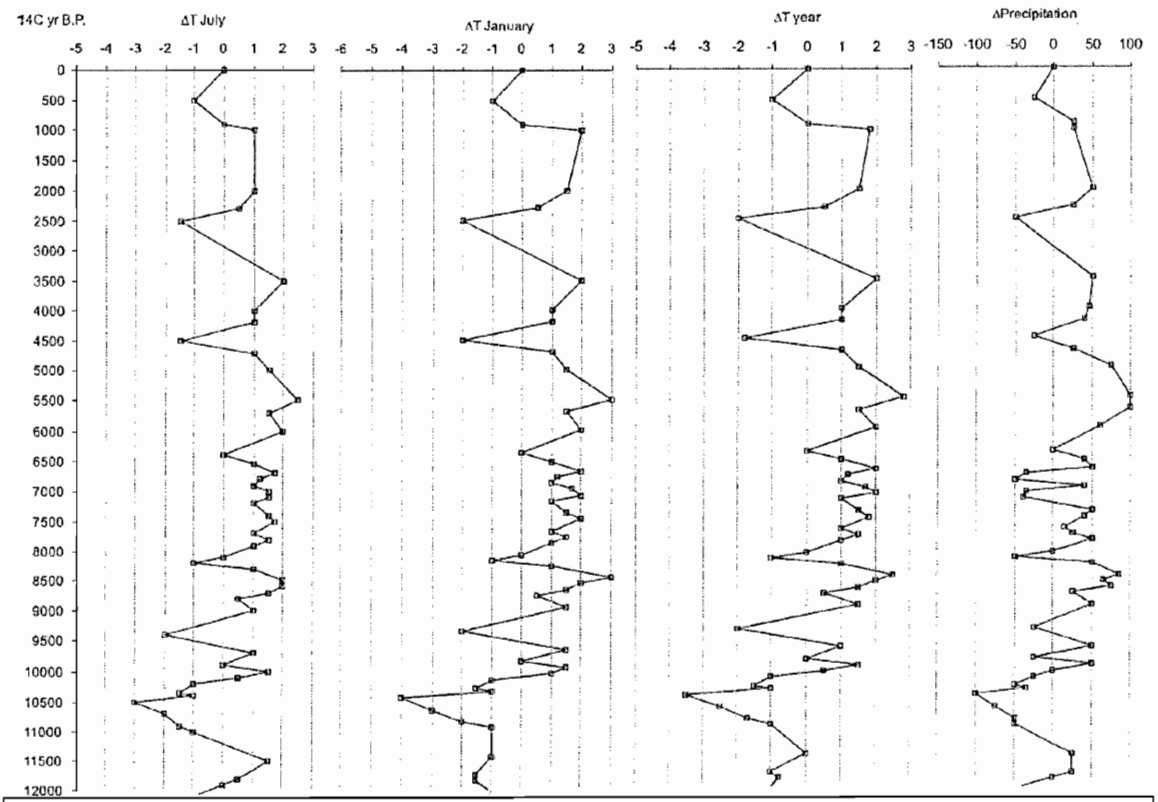

Figure 4.5- Averaged paleoclimate curve from Labaz Lake sites pollen (from Andreev et al, 2002)

4.6 Temperature Data

Vegetation based reconstructions of paleoclimate provide only estimates of January and July temperatures and only for selected time intervals. For my thaw-lake simulations, linear interpolations was used to infer temperatures for years between Andreev et al.'s [2000 and 2002] reconstructions. For example, with temperature data for every 250 years a linear increase (or decrease) was applied to extract data for years 0-249. A sinusoidal function was used to generate monthly temperatures using the January and July reconstruction to set the minimum and maximum monthly temperatures. The temperature anomalies were added to the average seasonal temperatures. These data are what drives the model.

4.7 Methane Calculation

Methanogenesis is the process where methane is produced by microbes from the metabolism of biomass. Microbes that produce methane as part of anaerobic respiration are called methanogens. Methanogensis is the final step in the break down of organic matter and occurs in conjunction with the fermentation processes (Thauer and Shima, 2006).

For this model, I use the CH_4 flux calculation from thawed organic rich peat (yedoma) developed by Plug and West [in preparation] which incorporates: lake size, yedoma carbon content, and decomposition efficiency the latter which was developed from Walters et al [2006]. The mean carbon content on the upper 50 m of yedoma, assuming it is undisturbed, is 26.8 kg C m^{-3} [Walters et al, 2006]. Of this 26.8 kg C m^{-3}, 16.5% is released through

methanogensis during thaw lake development. However, lake bottom deposits have 33% less carbon than virgin yedoma and methane production is 50% from cellulose decomposition as opposed to the result of methanogen activity [Walters et al, 2006]. The result is a flux of 4.3 kg CH_4 m^{-3} of permafrost thawed around the perimeter of the lake. The volume flux of permafrost thawed (m^3 y^{-1} lake $^{-1}$) is calculated by multiplying the area thawed in one year in the cross sectional model by the basin's perimeter that year.

The assumptions for this mass balance calculation are: lakes are expanding in yedoma that has not already undergone previous thawing (ie. virgin yedoma) and that methanogensis approaches instantaneous. Therefore the current flux depends on the current expansion rate. In reality, actual methanogensis is an ongoing process that can take several years.

5.0 RESULTS

The evolution through time of seven properties of the model lakes were examined: rate of radial of expansion, lake radius, rate of talik deepening, talik depth, volumetric thaw rate, annual methane released and cumulative methane released. For comparison, July and January temperatures for Taymyr and Labaz are displayed in Figure 5.1. On the graphs year 0 is at the start of the model, and the end of the graphs is present day.

5.1 Model Radial Growth

The Taymyr region displays an average annual expansion rate of about 0.02 m per year (Figure 5.2). The annual variation in the growth rate is up to 0.75 m in growth and 0.75 m of shrinkage, likely caused by intrinsic variability or high temperature fluctuation. The maximum radial increase occurs at approximately 7750 years ago and the maximum shrinkage occurs at 5000 years ago. There does not appear to be an overall climatic signal in the radial expansion rate.

The Labaz Lake region graph shows a higher average annual expansion rate than Taymyr, about 0.2 m per year (Figure 5.2). A maximum expansion of 1.1 m occurs at about 10 000 years ago. The maximum shrinkage occurs 7 000 years ago and is 0.6 m. In contrast to the Taymyr Peninsula there does seem to be an overall sinusoidal climate signal.

The lake radius growth graph shows that the Taymyr lake grew to a maximum radius of 230 m over the duration of the Holocene (Figure 5.3), compared to the Labaz lake which grew to 2100 m (Figure 5.3). The growth

curves for these lakes are also quite different. The Taymyr lake graph shows several pronounced "steps" during which time the lake stops expanding altogether. The first such step occurred between 10700-8500 years ago when the lake radius remained at about 40 m. The next hiatus in lake expansion occurred between 8000-6400 years ago when the radius remained constant at about 125 m. Between 5000-3750 years ago the lake radius was about 160 m. The last thousand years sees a decrease in the rate of lake growth, and the radius seems to peak at a value of 230 m.

The lake from the Labaz region shows a much smoother profile of lake expansion. Between 11000-10300 years ago the lake radius remained constant at 100 m. There are also a few other small "blips" that occur at 8400, 4700 and 2600 years ago when lake expansion slows down. It also does not increase as rapidly in the last few hundred years.

Taymyr **Labaz**

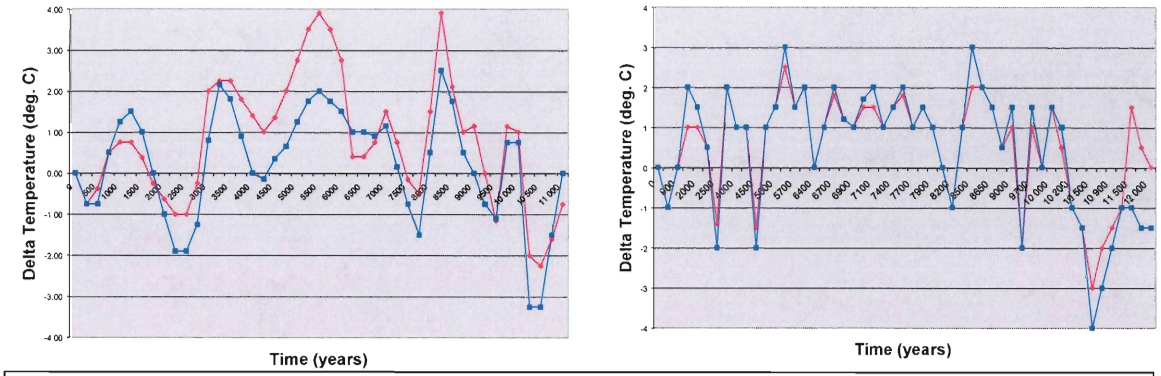

Figure 5.1-Averaged paleoclimate curve from fossil pollen-July red, January Blue (After Andreev 2000, 2002)

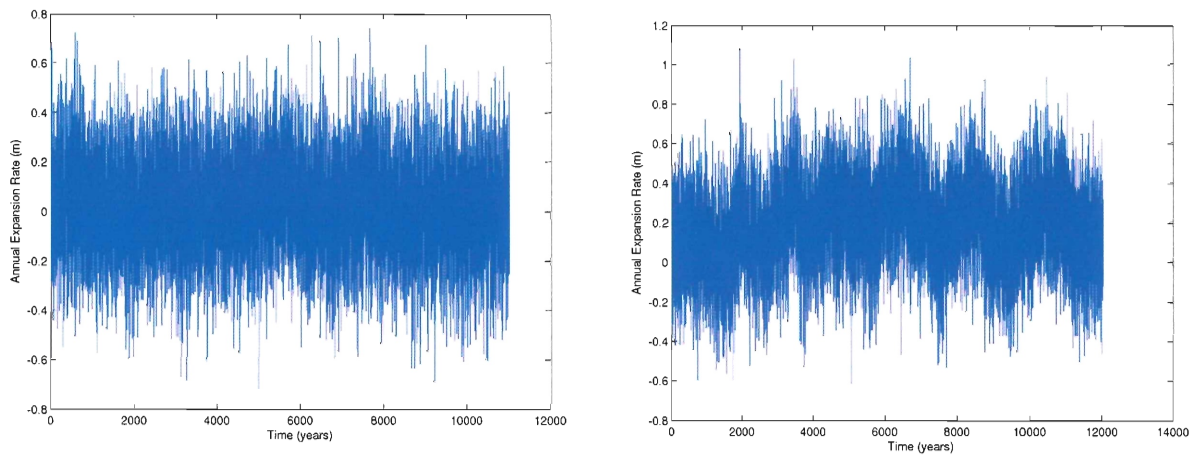

Figure 5.2- Annual expansion rate (m)

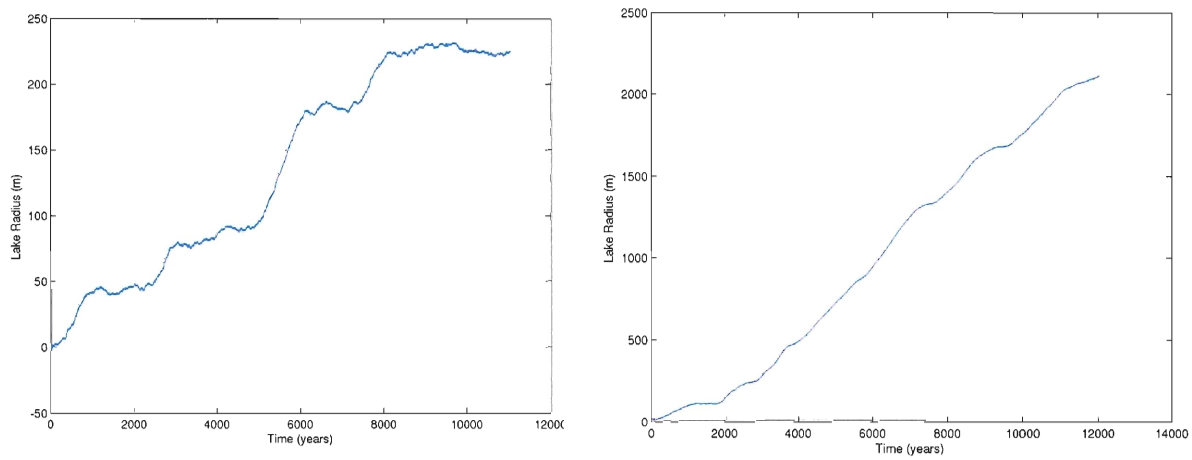

Figure 5.3-Total lake radius expansion (m)

5.2 Talik Growth

The Taymyr talik expands and shrinks by as much as 1.25 meters in the first 300 years of the model, from 11 000 to 10 400 years ago (Figure 5.4). This quickly decreases to about 0.25 m expansion or contraction and as the talik approaches dynamic equilibrium the rate levels out to 0.1 m expansion or contraction each year.

The Labaz lake shows a similar trend, initially deepening by as much as 0.9 m and shrinking by 0.75 m between 12 000 to 11 700 years ago (Figure 5.4). By about 7000 years the lake depth approaches stability.

The talik depth for the Taymyr lake eventually reaches 57 m (Figure 5.5). It initially shows a very sharp increase followed by a step wise increase, corresponding to the decline in lake radius expansion. The talik only increases by 3 m over the last 4000 years. The Labaz lake again shows a much smoother profile of talik depth against time (Figure 5.5). The talik for Labaz reaches 150 m. Small "bumps" in the graph correspond to stagnations in talik deepening.

Taymyr **Labaz**

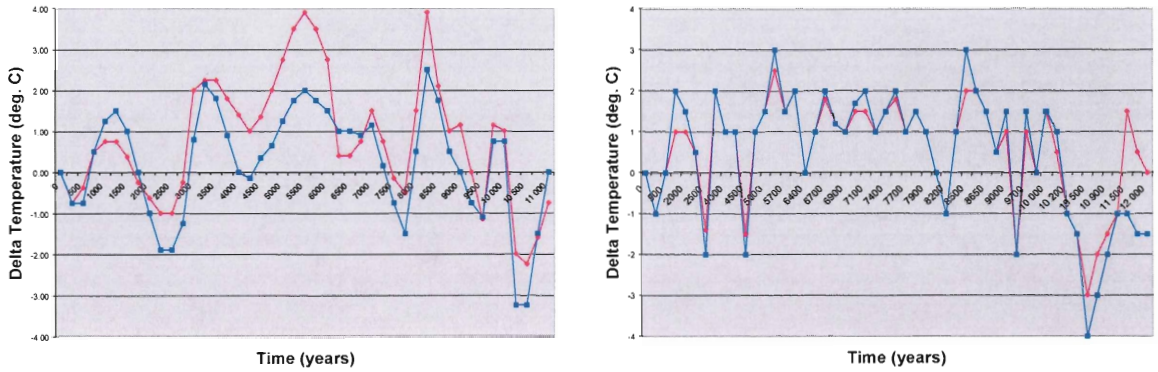

Figure 5.1-Averaged paleoclimate curve from fossil pollen (July red, January Blue)

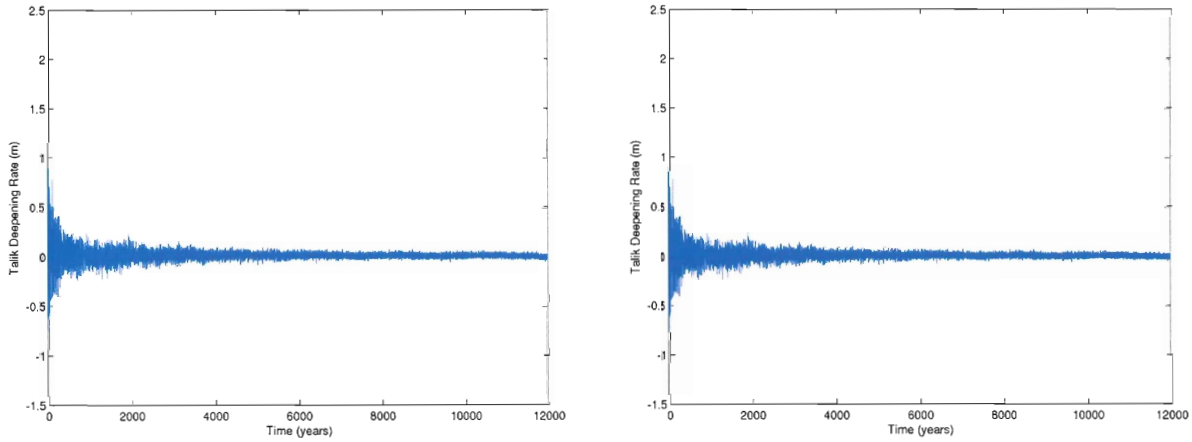

Figure 5.4- Talik deepening rate (m)

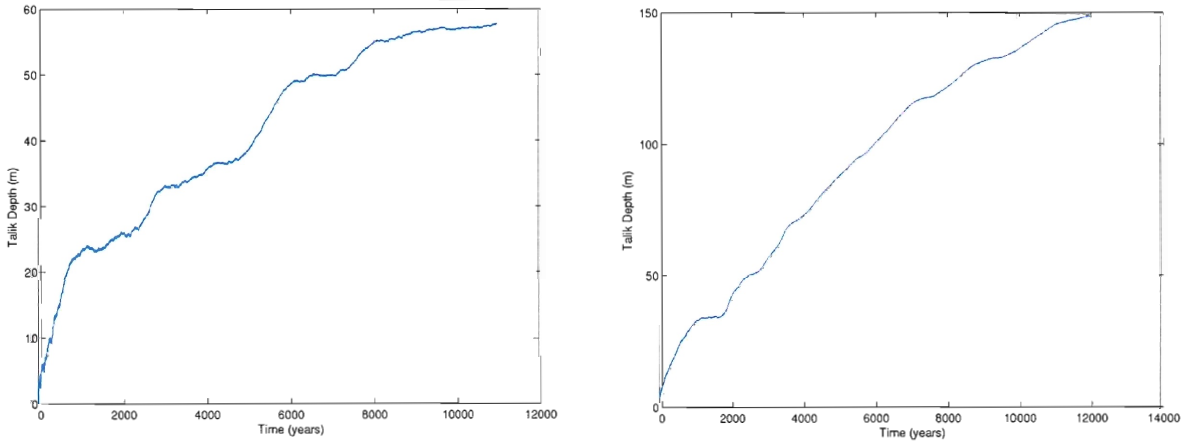

Figure 5.5- Talik depth (m)

5.3 Methane

The volumetric thaw rate (in m^3/yr) is extrapolated from the two-dimensional model to a three-dimensional lake using the increase in thawed cross-sectional area and assuming the lake is circular. The volumetric thaw rate broadly increases throughout the Holocene for both the Taymyr and Labaz lakes. It reaches a maximum of 5.0×10^3 m^3/yr approximately 4100 years ago for the Taymyr lake, but the average by the end of the model run was about 1.2×10^3 m^3/yr. The maximum volumetric thaw rate for the Labaz lake is 5.6 $\times10^3$ m^3/yr which occurred approximately 1600 years ago. The average attained was 1.3×10^3 m^3/yr.

To calculate methane release rate the volumetric thaw rate is multiplied by 4.63 kg CH_4/m^3, the product of methanogensis given the concentration of carbon in Siberian permafrost and the efficiency of methanogensis [Walter et al, 2006] (See Section 4.7). The methane release graph, in kg/yr for each region, is essentially the same shape as the volumetric thaw rate graph [Figure 5.6]. The maximum methane released in one year from Taymyr is 2.1×10^4 kg/yr 4100 years ago (Figure 5.6). The average methane release for the lake is 0.43×10^4 kg/year. The maximum for Labaz is 2.43×10^5 kg/yr, which occurred at 1600 years ago (Figure 5.6). This is a whole magnitude higher than Taymyr. The average annual methane release for the lake is about 0.5×10^5 m^3/yr.

Figure 5.7 is a graph of the cumulative methane release. For Taymyr the total methane released over the past 11 000 years is 10.3×10^6 kg (Figure 5.7). The total for the Labaz lake during the past 12 000 is an order of

magnitude greater, 12.3×10^7 kg (Figure 5.7). Over the past 11 000 years the Labaz lake releases 9.97×10^7 kg more than the Taymyr lake.

Taymyr **Labaz**

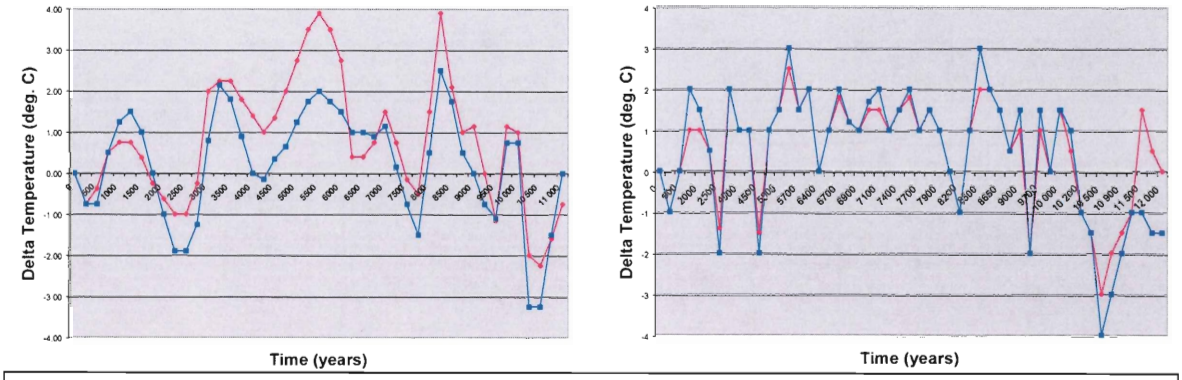

Figure 5.1-Averaged paleoclimate curve from fossil pollen (July red, January Blue)

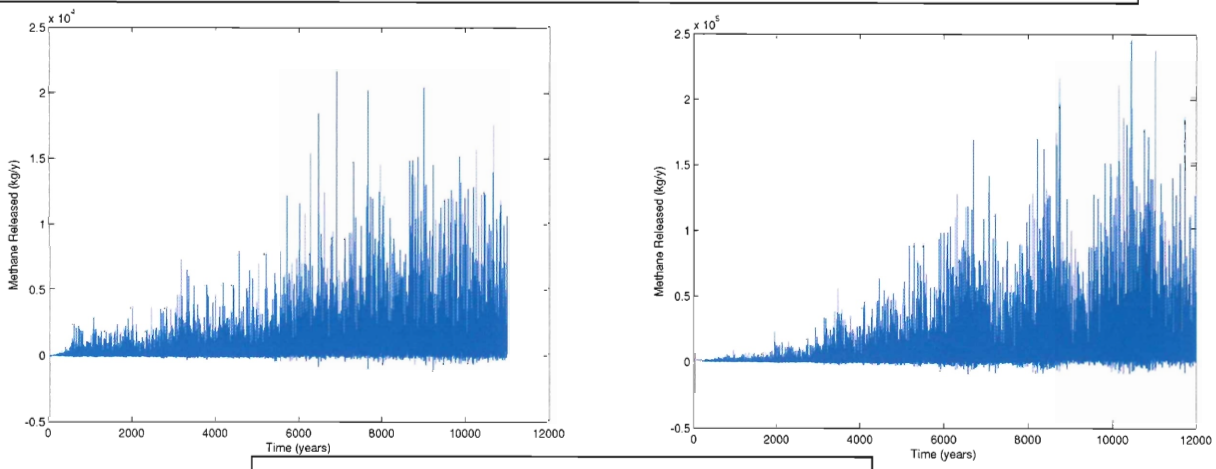

Figure 5.6- Methane released (kg/yr)

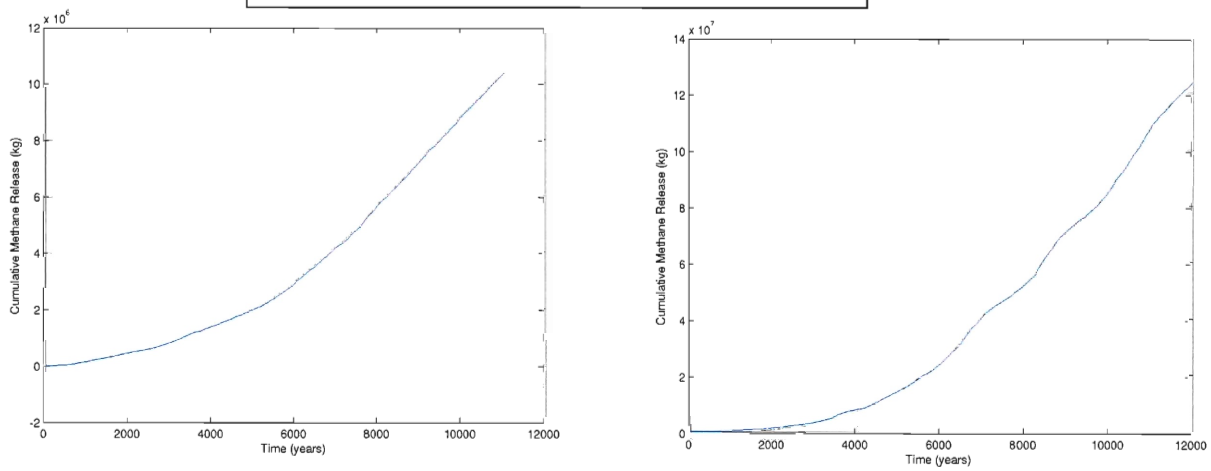

Figure 5.7-Cumulative methane release (kg)

5.4 Sources of Error and Limitations

A primary source of error is the temperature records used to drive the model. Though they are the most complete and have the highest resolution data available for Siberia, there is error associated with sampling as well as the statistical transfer functions the authors use, as stated by Andreev et al [2000, 2002].

One limitation in this study to predictions for thaw lake behaviours model is that I did not incorporate precipitation values into the model, but instead assumed that lake levels remained static throughout the Holocene. Lake level changes might influence the radial expansion and the quantity of material thawed, as significant thawing occurs at the water line of the lake. The reason that precipitation data was not incorporated into the model is that I could not find any studies linking precipitation fluxes to changes in lake level. Simply assuming all precipitation that fell into a basin ended up in a lake is not a reasonable assumption, as there will be losses from transpiration, evaporation, sublimation as well as other losses through the substrate.

Another limitation is that the model did not incorporate wave action within the lakes. The presence of orientated thaw lakes in some regions indicates that wave action might significantly increase erosion of lake margins [Carson and Hussey, 1962], particularly in large lakes like the one simulated at Labaz. Larger lakes may have more wave action, which equates to more rapid radial expansion. This parameter would be difficult to incorporate directly, but an estimate of lake erosion from waves could be conducted that would at

least indicate a magnitude of increase from wave action with an increasing lake size.

An additional limitation is that the substrate properties for both the Taymyr and Labaz where the same. Both had similar geothermal gradients, excess ground ice contents and organic content based on the assumption that both fall into the broad class of Siberian yedoma. Although it is unlikely that the two regions are identical in these properties, evidence to the contrary is lacking in the available literature. Moreover, the assumption of uniformity in Siberian yedoma has been used elsewhere [eg. Walter et al, 2006 and Zimov et al, 1997]. My results are best viewed as an illustration of the sensitivity of lakes to Holocene climate between two different regions.

6.0 DISCUSSION

6.1 Radial Growth and Talik Depth

The steps in the radius growth and talik growth graph, representing times of minimal increase, do correspond to particularly cold periods in the climate data [Figure 5.1]. Between 10 700 and 8500 the temperature was generally colder than the present average with small warming fluctuations. The next step between 8000-6400 the temperature was similar overall to the current average. Similarly between 5000-3750 years ago the temperature was actually warmer than present by 1- 2.75°C, yet the lake radius only increases minimally. The temperature between 2750-1750 years ago was between 0.25-1°C colder than current. This cooler period does show up as a plateau on the lake radius graph. Because the average July temperature is so low for Taymyr, even small decreases in the temperature seem to have pronounced effects on the growth of the lake. The talik depth graph shows an overall similar profile to the lake radius graph, though the plateaus are less pronounced. Because the talik is several meters below the surface and below the lake, it is less susceptible to changes in air temperature.

Between 11 000-10 200 years ago the temperature was between -1 to -3°C colder than average at Labaz. This corresponds to the first and most pronounced step in the lake radius and talik depth graphs. The other smaller steps at 8400, 4700 and 2600 years ago also correspond to times when the temperature was at or below the current average [Figure 5.1]. This indicates that the current average summer temperature is just on the fringe of being warm enough to create significant active thaw.

The radial growth and talik depth graphs both show that Labaz lake grew larger than Taymyr lake. This is not surprising considering that the Labaz region has a July temperature of 10-12°C, compared to 4-6°C in Taymyr. It is surprising, however, that the 5°C difference between Labaz and Taymyr resulted in a difference of 9 times in lake radius and 2.6 times in talik depth. From this we can conclude even small geographical distances can have large implications for climate variability, and thus the size thaw lakes can attain. For any regional study to be completed on the amount of methane released from Siberia, a comprehensive study would need to be completed to fully understand the paleoclimate dynamics of Siberia.

It is also important to note that these lakes reach sizes on the size of lakes observed in nature by West and Plug and Plug and West. Most lakes would probably not reach the size of Labaz as landscapes are not infinitely flat and the lake would likely drain or run out of ice-rich permafrost after some period of time.

6.2 Methane Release

Assuming Taymyr and Labaz are two bracketing conditions for Siberia (Taymyr being the coldest climate and Labaz being the warmest) we can calculate the quantity of methane released in the atmosphere during the Holocene. Using an estimate of 1 million km^2 of Siberia covered by 20% thaw lake area, each with an average radius of 1km (Plug and West, in preparation), there are about 63 700 lakes in Siberia. Multiplying that number by the total methane released from the Taymyr region I get a value of 6.56×10^{11} kg (656

teragrams) of methane released during the last 11 000 years. Then taking the same amount of lakes but applying it to the Labaz scenario I get a value of 7×10^{12} kg (7000 teragrams) of methane released.

To compare the total methane production in one year from all the lakes in Siberia to the current global production of methane, 600 Tg per year (IPCC, 2006), I took the maximum amount of methane produced in one year from Taymyr, 2.1×10^{4} kg/yr, converted it to Tg and multiplied it by the number of lakes, 63 700. This equals 1.34 Tg of methane per year, which is about 0.22% of the global annual production. The mean methane production for the Holocene, however, was 2.6×10^{3} kg/yr per lake which translate to 0.17 Tg per year, or 0.03% of methane production for one year.

For the Labaz scenario the maximum amount of methane produced in one year is 2.43×10^{5} kg/yr. This equals 15.5 Tg per year if extrapolated to lakes in Siberia. This is 2.6% of the global annual production. The mean production was 0.36×10^{5} kg/yr per lake, or 2.29 Tg per year for Siberia in one year. This is 0.38% of the yearly global production of methane.

As a final step I compared these estimated values of methane production from Siberian thaw lakes to other sources of methane (Figure 6.1). Thaw lakes contribute on the scale of other natural sources, such as termites and ocean hydrates, but are small compared to all of the anthropogenic sources. However, if other regions in Siberia are warmer than Labaz then thaw lakes could be contributing at least on a hemispheric level, perhaps even global, to methane concentrations.

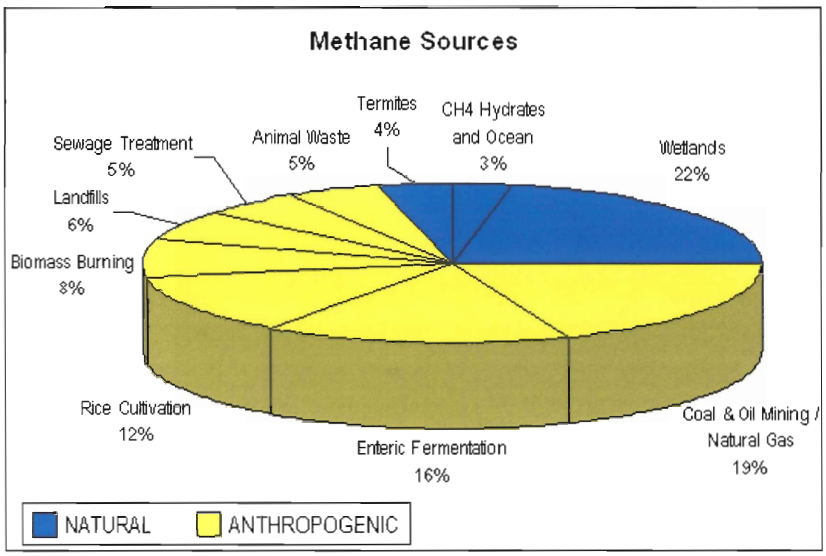

Figure 6.1- Natural and Anthropogenic Sources of Methane (from Goddard Institute for Space Studies, 2004)

7.0 CONCLUSIONS AND FUTURE WORK

My results show: 1) Climate data for Taymyr and Labaz regions indicate that currently climate within Siberia is different over small geographic distances at present and also responded differently throughout the Holocene. 2) Thaw lake model simulations demonstrate that temperature fluctuations of a few degrees can have large implications for the growth of lakes, and can result in thousand year long periods of stability. 3) Model simulations also demonstrate that thaw lakes are a source of methane at the global scale. The dynamics and behaviour of thaw lakes over the Holocene indicate that thaw lakes also might act as positive feedback to global warming over the next few centuries.

This model is a good first approximation of how thaw lakes behaved during the Holocene. In order to have a more comprehensive understanding the following might be completed: 1) Both precipitation and wave action might be incorporated into the model. A more thorough review of literature could reveal how lake levels change over time to precipitation fluctuations. Alternatively, develop a model basin and applying evaporation and transpiration values and measuring how lake levels change within the model. Incorporating wave action would likely need substantial field research that would focus on lake size and the percentage of erosion that occurred from wave action. This would at best only be an approximation.

2) Instead of using pollen reconstructions one could use a meso-scale general circulation model. At present there is one such model, the FAMOUS model from the Hadley Centre, but it is yet to be completed for Siberia. By

using the data from the FAMOUS model to drive the thaw lake model one could take the methane output from each year and feed it back into FAMOUS and use it drive further changes. This could help assess the degree to which methane acts as a positive feedback system.

3) Ice core data from the Taylor Dome and Greenland have yielded methane curves for the last several thousand years (Brook, 2003). The cumulative methane curves from Taymyr, Labaz and other regions, as predicted by the model, might be compared to these ice-core methane records to test the hypothesis that thaw-lakes have influenced methane at the global atmospheric scale during the Holocene.

8.0 REFERENCES

Andreev, A.A., Klimanov, V.A. 2000. Quantitative Holocene climatic reconstruction from Arctic Russia. *Journal of Paleolimnology*, 24, 81-90.

Andreev, A.A., Siegert, C. 2002. Late Pleistocene and Holocene Vegetation and Climate on the Taymyr Lowland, Northern Siberia. *Quaternary Researchl, 57, 138-150.*

Andreev, A.A., Tarasov, P.E., Klimanov, V.A., Melles, M., Lisitsyna, O.M., Hubberen, H.-W. 2004. Vegetation and climatic changes around the Lama Lake, Taymyr Peninsula, Russia during the Late Pleistocene and Holocene. *Quaternary International*, 122, 69-84.

Berger, A., Loutre, M.F. 1991. Insolation values for the climate on the last 10 million years. *Quaternary Science Reviews* 10, *297-318.*

Blunier, T., Chappellaz, J., Schwander, J., Stauffer, B., Raynaud, D. 1995. Variations in atmospheric methane concentration during the Holocene epoch. *Nature* 374, 46-50.

Brewer, M., Carter, M., Glenn, R. 1993. Sudden Drainage of of a thaw lake on the Alaskan costal plain, in *Sixth International Conference on Permafrost*, edited by G. Zhou.

Briner, J.P. et al. 2006. A multi-proxy Lacustrine record of Holocene climate change on northeastern Baffin Island, Arctic Canada. *Quaternary Research* 65, 431-442.

Brook, E. 2003. Taylor Dome and Greenland Ice Core Methane and Interplanetary Dust Data. Boulder, CO: National Snow and Ice Data Center. Digital Media.

Brown, R.J.E. 1970. *Permafrost in Canada; its influence on northern development*. Toronto: University of Toronto Press.

Burn, C.R. 1997. Cryostratigraphy, paleogeography and climate change during the early Holocene warm interval, western Arctic coast, Canada. *Canadian Journal of Earth Science* 23, 79-803.

Burn, C.R. 2002. Tundra Lakes and permafrost , Richards Island, western Arctic coast, Canada. Canadian Journal of Earth Sciences, 39, 1281-1298.

Burn, C.R, and Smith, M.W. 1988. Thermokarst lakes in Mayo, Yukon Territory, Canada, in *5th International Conference on Permafrost, Proceedings*, vol. 5, edited by K. Senneset, pp. 700-705.

CAPE, 2001. Holocene paleoclimate data from the Arctic: testing models of global climate change. *Quaternary Science Reviews* 20, 1275-1287.

Chapin III, F.S et al. 2005. Role of Land-surface changes in Arctic summer warming. *Science* 310, 657-662.

Clark, P.U., Marhsall, S.J., Clarke, G.K.C., Hostetler, S.W., Licciardi, J.M., Teller, J.T., 2001. Freshwater forcing of abrupt climate change during the last glaciation. Science *293*, 283-287.

COHMAP, 1998. Climate changes of the last 18 000 years: observations and model simulations. *Science* 241, 1043-1052.

Davis, N. 2001. Permafrost: A Guide to Frozen Ground in Transition. University of Alaska Press, Fairbanks, Alaska.

Dyke, A.S., James, H., Savelle, J.M. A history of sea ice in the Canadian arctic archipelago based on postglacial remains of the bowhead whale (*Balaena mysticetus*). *Arctic* 49, 235-255.

Dyke, A.S., Savelle, J.M. 2001. Holocene history of the Bering Sea bowhead whale (*Balaena mysticetus*) in its Beaufort Sea summer grounds off southwestern Victoria Island, Western Canadian Arctic. *Quaternary Research* 55, 371-379.

Einstein, Norman. 2005. Location of the Laptev Sea north of Siberia, Russia. Taymyr Peninsula, Wikipedia [online]. Available from http://en.wikipedia.org/wiki/Taymyr_Peninsula. [Cited 11 March 2006]

Environmental Protection Agency (EPA). Methane: Science [Online]. Available from http://www.epa.gov/methane/scientific.html. [Cited 11 March 2006].

French, H.M. *The Periglacial Environment*, Second Edition. Essex: Addison Wesley Longman, 1996.

Gajewski, K., Garalla, S. 1992. Holocene vegetations histories fro three sites in the tundra of northwest Quebec, Canada. *Arctic and Alpine Research* 24, 329-336.

Gajewski, K. Payette, S. Ritchie, J.C.1993. Holocene vegetation history at boreal forest-shrub tundra transition in northern Quebec. *Journal of Ecology* 81- 433-443.

Gildor, H., Tziperman, E. 2001. A sea climate switch mechanism for 100-kyr glacial cycles. *Journal of Geophysical Research* 106, 9117-9133.

Goddard Institute for Space Studies. 2004. Education: Global Methane Inventory-The Global Methane Cycle. Available from http://icp.giss.nasa.gov/education/methane/intro/cycle.html. [Cited 10 March 2007].

Goetcheus, V.G., Birks, H.H. 2001. Full-glacial upland tundra vegetation preserved under tephra in the Beringia National Park, Seward Peninsula, Alaska. Quaternary Science Reviews, 20, 135-147.

Grave, N.A. 1968. The earth's permafrost beds [Merzlyye tolshchi zemli]. Canada Defense Research Board Translation $T_{499}R$, 1-10.

Hinkel, K.M., Frohn, R.C., Nelson, F.E., Eisner, W.R., and Beck, R.A. 2005. Morphometric and spatial analysis of thaw lakes and drained thaw lake basins in the western Arctic Coastal Plain, Alaska. Permafrost and Periglacial Processes, 16, 327-341.

Hopkins, J.M. 1949. Thaw lakes and thaw sinks in the Imuruk Lake area, Seaward Peninsula, Alaska. Journal of Geology, 57, 119-131.

Howard, A. 1997. Badland morphology and evolution: interpretations using a simulation model. *Earth Surface Processes and Landforms* 22, 211-227.

Indermühle, A., Stocker, T/F, Joss, F., Fischer, H., Smith, H.J., Wahlen, M., Deck, D., Mastroianni, D., Tschumi J., Blunier, T., Meyer, R., Stauffer, B., 1999. Holocene carbon-cycle dynamics based on CO_2 trapped in ice at Taylor Dome, Antarctica. *Nature* 398,121-126.

Intergovernmental Panel on Climate Change (IPCC) [online]. 2006. Available from http://www.ipcc.ch/. [cited 10 March 2006].

Kaufman, D.S., et al. 2004. Holocene Thermal Maximum in the Western Arctic (0-180° W). *Quaternary Reviews* 23, 529-560.

Kaplan, M.R., Wolfe, A.P. 2006. Spatial and temporal variability of Holocene temperature in the North Atlantic Region. *Quaternary Research* 65, 223-231.

Kutzbach, J.E.1981. Monsoon climate of the early Holocene: climate experiment with Earth's orbital parameters for 9000 years ago. *Science* 214, 59-61.

Lachenbruch, A.H. 1962. Mechanics of thermal contraction cracks and ice-wedge polygons in permafrost. *Special GSA paper* 70, 69.

Lachenbruch, A.H. 1966. Contraction theory of ice wedge polygons; a qualitative discussion. In : *Proceedings of, 1st International Conference on Permafrost*. National Academy of Science, National Research Council of Canada, Publication 1287, 63-71.

LANDSAT [online]. Available from landsat.org. [Accessed 10 March 2006].

Licciardi, J.M., Teller, J.T., Clark, P.U.1999. Freswater routing by the Laurentide Ice Sheet during the last deglaciation. In: Clark, P.U. Webb, R.S., Kerigwin, L. (eds), Mechanisms of Glocal Climate Change at Millenial Time Scales, Geophysical Monograph Series 112. American Geophysical Union, Washington, DC, pp 177-201.

McCulloch, D., Hopkins, D.M.1966. Evidence for an early recent warm interval in northwestern Alaska. *Geological Society of America Bulletin* 77, 1089-1108.

MacKay, J.R. 1973. The growth of pingos, western Arctic coast, Canada. *Canadian Journal of Earth Science*. 10: 979-1004. **In:** Ritter, D.F., Kochel, R.C., Miller, J.R. Process Geomorphology, Fourth Edition. New York: McGraw Hill, 2002.

MacKay, J.R. 1981. An experiment in lake drainage, Richards Island, Northwest Territories; A progress report, *Current Research*, Part A, *Geological Survey of Canada*, 81, 63-68.

MacKay, J.R. 1988. Catastrophic Lake Drainage, Tuktoyaktuk Peninsula area, District of Columbia, Current Research, Part D, Interior Plains and Arctic Canada, *GSC*, 88, 93-90.

Rampton, V.N. 1988. Quaternary geology of the Tuktoyaktuk coastlands, Northwest Territories, *Memoir 423*, Geological Survey of Canada.

Plug, L.J., and West, J.J. Thaw lake expansion in a two-deminsional coupled model of heat transfer and mass movement. *Accepted*.

Plug, L.J. and West, J.J. Expansion of permafrost lakes and resultant CH_4 flux under a warming climate. *In Preparation*.

Roering, J.J., Kircher, J.W., and Dietrich, W.E. 2001. Hillslope evolution by nonlinear, diffusive sediment transport on hillslopes and implications for landscape morphology. *Water Resources Research*, 35, 853-870.

Schwamborn, G.J., Dix, J.K., Bull, J.M., and Rachold, V. 2002. High-resolution seismic and ground penetrating radar-geophysical profiling of a thermokarst lake in the western Lena Delta, Northern Siberia. Permafrost and Periglacial Processes, 13, 251-318.

Scott and Plug, L.J. 2006. Thermokarst lake changes in continuous permafrost, Tuktoyaktuk Peninsula, Western Canadian Arctic. *In review Geophysical Research Letters*.

Spear, R.W.1993. The palynological record of Late-Quaternary Arctic tree-line north-western Canada. *Review of Palaeobotany and Palynology* 79, 99-111.

Thauer R.K., Shima, S.S. 2002. Biochemistry: Methane and microbes. *Nature* 440, 878-879.

Tomirdario, S.V. 1982. Evolution of lowland landscapes in northeast Asia during the late Quaternary time, in Paleoecology of Beringia, edited by D.M. Hopkins, 29-37, Academic Press, New York.

University of Texas Libraries. 2007. Canada-Shaded Relief Map [online]. Accessed April 25, 2007. Available from <www.lib.utexas.edu/maps/americas/canada_rel97.jpg>

Vardy, S.R., Warner, B.G., Aravena, R. 1997. Holocene climate effects on the development of peatland on the Tuktoyaktuk Peninsula, Northwest Territories. *Quaternary Reseach* 43, 90-104.

Washburn, A.L.1980. Geocryology; A survey of periglacial processes and environments. Halsted Press, a division of John Wiley & Sons Inc., New York.

West, J.J. and Plug, L.J. 2007. Time-dependant morphology of thaw lakes and taliks in deep and shallow ground ice. *Accepted*.

Walter, K.M., Zimov, S.A., Chanton, J.P., Verbyla, D., Chapin, F.S. 2006. Methane bubbling from Siberian thaw lakes as a positive feedback to climate warming. Nature, 443, 71-75.

Williams, Peter, J., and Smith, Michael, W. 1989. The Frozen Earth: Fundamentals of Geocryology. Cambridge Press, Oxford, Great Britain.

Woller, M.J. et al. 2004. Quantitative paleotemperature estimates from of chironomid head capsules preserved in arctic lake sediments. *Journal of Paleoliminology* 31, 267-274.

Zimov, S. Voropaev, Y., Semiletov, I., Davidov, S., Prosiannikov, F., Chapin III, F., Trumbore, S., Tyler, S. 1997. North Siberian lakes: A methane source fuelled by Pleistocene carbon. *Science* 277, 800-802.

Zoltai, S.C. 1995. Permafrost distribution in peatlands of west-central Canada during Holocene warm period 6000 years B.P. *Géographie Physique et Quaternarie* 49, 45-54.